Journal Pre-proof

Adaptive Non-Linear High Gain Observer Based Sensorless Speed Estimation of an Induction Motor

Abderrahmane Kadrine , Zoheir Tir , Om P. Malik ,
Mohamed A. Hamida , Alberto Reatti , Azeddine Houari

Please cite this article as: Abderrahmane Kadrine , Zoheir Tir , Om P. Malik , Mohamed A. Hamida , Alberto Reatti , Azeddine Houari , Adaptive Non-Linear High Gain Observer Based Sensorless Speed Estimation of an Induction Motor, *Journal of the Franklin Institute* (2020), doi: https://doi.org/10.1016/j.jfranklin.2020.06.013

Adaptive Non-Linear High Gain Observer Based Sensorless Speed Estimation of an Induction Motor

Abderrahmane KADRINE, Zoheir TIR, Om P. MALIK, Mohamed A. HAMIDA, Alberto REATTI and Azeddine HOUARI

Zoheir TIR
Corresponding author
Dept. of Electrical Engineering, University of El-Oued, Algeria.
Phone: 00 213 675 107 376 / **E-mail**: tir-zoheir@univ-eloued.dz

Abstract − An efficient sensor-less speed estimator, based on an adaptive non-linear high gain observer (HGO) which uses only the measured stator currents and control voltages in the presence of measurement noise, is proposed to estimate the speed of an induction motor. The proposed observer is an improved version of the common HGOs proposed in the literature. The observer gain, involving the use of a scalar time-varying design parameter governed by the Riccati differential equation, guarantees the best compromise between the fast convergence of the states and noise rejection with such adaptation of gains that the internal states of the observer exert low influence during the transient period and thus prevent system peaking. The design methodology of the proposed observer is given and its stability is studied. Results of simulation studies demonstrate that robustness and efficiency of the proposed observer are maintained under critical operating conditions, even where the efficiency of the fixed gain observer is decreased.

Keywords: Induction motor; Adaptive non-linear high gain observer; Measurement noise; Peaking phenomenon; Riccati equation; Tikhonov's regularization.

Introduction

High performance sensor-less speed control of induction motors (IMs) has received a lot of attention in recent years because speed estimation design and resultant control are challenging. Yet, eliminating the rotor encoder results in lower system cost, improved reliability and reduced sensitivity to electromagnetic noise. Ongoing research has focused on replacing the rotor encoder to produce sensor-less drives without altering the dynamic performance of the drive. Two methods, one based on injection of high frequency signal and the other on machine models [1], have been used to estimate the speed of the sensor-less drives. Methods based on the injection of high frequency signals are insensitive to some parameter variations and allow for an accurate estimation of the shaft speed at zero and low stator frequencies, but they generate high frequency noise degrading the system performance [1, 2]. In the high or medium speed range, machine model based methods allow for an accurate estimation of speed or position [1]. The scheme presented in this paper belongs to the methods based on machine models.

Further research continues to improve the reliability of the drive operation based on machine model methods in the zero to very low speed range [3]. Luenberger method is one of the most representative methods in this area [4]. Several sensor-less speed estimation methods for IM drives have been proposed in the literature [1-3, 5-26].

Sliding Mode Observer (SMO) [5] based speed estimation method is motivated by finite time convergence and robustness considerations. However, it results in chattering problems. Moreover, this method is difficult to implement, because its gain comprises the sign function and other design parameters whose values must be updated when previously unknown singularities occur [2, 11]. It is also sensitive to measurement noise [8, 10]. Furthermore, it leads to lack of accuracy of speed estimation under unobservable conditions in the zero speed region as reported in [18].

Extended Kalman Filter (EKF) [27] is mainly motivated by its implementation simplicity and robustness to noise generated in the system. However, it suffers from the lack of guaranteed stability [6, 8, 9]. Moreover, the EKF technique is valid for a limited range around the operating point, which limits its dynamic performance. It also frequently requires a large amount of real-time calculations [28]. It is

also more sensitive to variations in IM parameters, which can significantly lead to inaccuracy of speed estimation under unobservable conditions at zero or low speed region. Another important challenge of this technique is its instability under regenerating conditions [17]. Furthermore, it fails to offer satisfactory compromise between the robustness to measurement noise and estimation bandwidth [20].

The speed estimation method based on Adaptive Full-order Observer (AFO) from the currents and/or voltages errors, is well recognized in many studies of the speed sensor-less IM drives [14-16]. However, the drawback of this technique is its instability when rotor speed is close to zero in the regenerative region, even when the measurement noise and parameter errors are not considered [15]. This method also results in an error between the actual and estimated speeds [14].

Model Reference Adaptive System (MRAS) [21] based speed estimation method is one of many promising techniques used for sensor-less IM drives, due to its easy implementation, robustness and low computational complexity [17, 19, 21]. However, this technique has some drawbacks, such as complexity in the design of the adaptation mechanism block and sensitivity to uncertainty in the reference model [19]. Such drawbacks may lead to destabilization of the system during the regenerative mode of operation [22].

Use of interconnected form-based cascade observers to estimate the state of IM using stator currents and voltages is proposed in [23]. Based on that, a cascade observer interconnected to an estimator for the sensor-less speed estimation of an IM is proposed in [24]. In the same work, a high gain observer connected to an estimator is also studied to reconstruct the states of IM based on the design methodology proposed in [29]. Both techniques are tested and compared under the same conditions of operation in [24]. To remedy the problem of undesirable behavior that occurs at very low value of speed, the authors proposed a solution by modifying the observer gains following the observability property of IM, which switches the mode of the observer into an estimator. However, numerous complications related to this special methodology of design, such as switching the gains parameters, trigger threshold, and peaking of system, are the design problems that need to be avoided as stated in [30, 31]. Again, the main drawback of the interconnected observers lies in the difficulty of their implementation and calibration. Indeed,

computational complexity due to their gains which necessitates the solution of eighteen differential equations and its expression is mentioned in [10]. Moreover, the interconnected observer still suffers from the drawback that its gains are large enough when the IM is operated under unobservability conditions as reported in [24].

High Gain Observer (HGO) technique based on canonical form [32] has gained ample importance for sensor-less IM drives. Without measurement noise, this observer has the capability to rapidly reconstruct the system states and reject modeling uncertainty [33]. The HGO based on canonical form design is primarily motivated by its inherent simplicity. Moreover, the HGO tuning is realized via a single design parameter. For a survey of high gain observers, refer to [34] and the references therein.

HGOs also reveal that a trade-off exists between the sensitivity of measurement noise and quick convergence [35-37]. Based on this trade-off, the gain should be increased in a transient period to attain a quick reconstruction of the system states, because the effect of measurement noise is small enough. On the other hand, the reduction of the gains allows the internal states of observer to exert low influence during the transient period and thus prevent system peaking [31, 35, 38]. Indeed, as reported in [36, 39-42], by reducing the observer gains, the so-called "peaking phenomenon" of the internal states of the observer, that may be exhibited during the transient period and may lead to destabilization of the system, will be avoided. Yet it solves the challenging problem of numerical implementation present in standard high gain observers because during digital implementation, signals and parameters must be represented in the finite word length of the digital system. To deal with this trade-off, many studies in the literature have sought to improve the standard version of HGOs [31, 35, 37, 38, 43, 44].

The effects of high-frequency measurement noise in high gain observer for sensor-less speed control of IMs have not been fully investigated yet. Nevertheless, noises are inevitably produced through the harmonics of the stator current and voltage signals, and the wide-band harmonic content coming from the non-sinusoidal power supplies, such as Pulse Width Modulation (PWM) converters [45].

A high gain observer with fixed gain based on a triangular observable form that uses only the measured stator currents, control voltages and rotor speed for the on-line estimation of internal states

(load torque and rotor flux) and time varying parameters (rotor resistance and/or stator resistance) is proposed in [46, 47].

Significant effort is spent in [8, 10, 20] to approximate the standard high gain observer with fixed gains for sensor-less speed estimation of an IM by exploiting a suitable procedure to tackle the singularities occurring whenever the observability is lost at zero and very low speeds. However, as shown in [8, 10, 20], the approximate observer still suffers from the so-called peaking phenomenon, high-frequency oscillation and large uncertainties especially in the unobservable regions. Indeed, as mentioned in [20, 36, 37, 39], such drawbacks are due to the very large value of the observer gains which remain unchanged even in the presence of noise. Moreover, authors in [8, 10] use a limited type of high gain observer which is based on the system structure assuming a complete triangular observable form in which the dynamics of non-linear part of the system have triangular state dependence. It means that certain non-linear state-dependent terms are treated as external disturbances to guarantee that the dynamics of the system admit the triangular observable form. Indeed, such a treatment inevitably leads to a conservative design as reported in [48].

An extension to this work, in which the authors attempt to overcome some of the aforementioned drawbacks, is considered in [25], but it is not a complete study. The studied techniques are not deeply detailed, the noise measurement is not taken into account and no comparative analysis with standard observer is studied. Moreover, the authors do not include any detailed study of the Jacobian matrix inverse to tackle the singularities occurring during the operation of the IM, and the analysis of state estimation convergence of the proposed observer is not included.

Motivated by the above discussion and inspired by the aforementioned works, the principal aim of this paper is to investigate the observation of the IM states in the presence of measurement noise by using a nonlinear high gain observer based on the canonical form. The gains are updated on-line governed by a Riccati Differential Equation (RDE) to get an acceptable compromise between the accuracy of the observer and its sensitivity to measurement noise, and the peaking phenomenon of the internal states of the observer during the transient period. The significant contributions of this work are highlighted below:

- o   the proposed adaptive nonlinear high gain observer is used for sensor-less speed estimation of IMs taking into account the high-frequency measurement noise.

- o   to overcome the manifestation of trade-off that exists between the sensitivity of measurement noise, and quick convergence, and peaking phenomenon, the gains are updated on-line governed only by the RDE;

- o   the proposed observer has a numerical implementation advantage compared to the standard high gain observer because the updated gains mostly have low value during the operation of the observer. Reduction in the size of the reversible Jacobian matrix also greatly simplifies the computational complexity.

- o   the proposed observer is based on a large class of nonlinear and non-triangular observable forms that are observable for any input that allow designing nonlinear observers to estimate the unknown inputs as well as the state variables at the same time.

- o   an approximation approach based on a suitable technique called Tikhonov's regularization [49] is introduced to implement the proposed observer which requires the inversion of the Jacobian matrix to regulate in almost any region of operation because the induction motor may operate in its unobservable domain;

- o   in the framework of an industrial benchmark stated in [13], the trajectories have been used to test and evaluate the performance of the proposed observer when the IM remains in the unobservable conditions such as in the zero to very low speed range;

- o   the validity of the proposed observer is confirmed also by its comparison with the standard high gain observer which has been performed by using a constant value for the gain parameter [8, 10, 20] .

The rest of the paper is structured as follows. The problem formulation is set in Section 2. The mathematical model and the IM observability analysis are provided in Section 3. Design and application of the nonlinear adaptive high gain observer for sensor-less speed estimation of IMs are described in

Section 4. The convergence analysis of the proposed observer and results of simulation studies are presented in Sections 5 and 6, respectively. The conclusions are given in Section 7.

Problem formulation

Based on their models in the fixed frame α-β axes, observers are designed to get the information of initial rotor position of the IM. Considering the load torque as an element of the state vector, the IM dynamic model is described as:

$$\dot{\zeta} = f(\zeta, u)$$
$$y = h(\zeta) + \ell \tag{1}$$

where,

$$\dot{\zeta} = \begin{bmatrix} i_{s\alpha} \\ \phi_{r\alpha} \\ \phi_{r\beta} \\ i_{s\beta} \\ \dot{\Omega} \\ \dot{T}_l \end{bmatrix}, f(\zeta, u) = \begin{bmatrix} -K_1 i_{s\alpha} + K_2 \phi_{r\alpha} + K_3 \Omega \phi_{r\beta} + m v_{s\alpha} \\ K_4 i_{s\alpha} - K_5 \phi_{r\alpha} - p\Omega \phi_{r\beta} \\ K_4 i_{s\beta} + p\Omega \phi_{r\alpha} - K_5 \phi_{r\beta} \\ -K_1 i_{s\beta} - K_3 \Omega \phi_{r\alpha} + K_2 \phi_{r\beta} + m v_{s\beta} \\ K_6(\phi_{r\alpha} i_{s\beta} - \phi_{r\beta} i_{s\alpha}) - K_8 T_l - K_7 \Omega \\ 0 \end{bmatrix}$$

and, $v_{s\alpha}, v_{s\beta}, i_{s\alpha}, i_{s\beta}, \phi_{r\alpha}, \phi_{r\beta}, \Omega$ and T_l are the stator voltage inputs, stator currents, rotor fluxes, rotor angular speed and load torque, respectively. Subscripts r and s refer to the rotor and stator, respectively.

The parameters K_i for $i \in [1, 8], \sigma, T_r$ and m are $K_1 \stackrel{\text{def}}{=} \frac{1}{\sigma L_s}\left(R_s + \frac{M^2}{T_r L_r}\right), K_2 \stackrel{\text{def}}{=} \frac{1}{\sigma L_s}\left(\frac{M}{T_r L_r}\right), K_3 \stackrel{\text{def}}{=} \frac{P}{\sigma L_s}\left(\frac{M}{L_r}\right), K_4 \stackrel{\text{def}}{=} \frac{M}{T_r}, K_5 \stackrel{\text{def}}{=} \frac{1}{T_r}, K_6 \stackrel{\text{def}}{=} \frac{pM}{JL_r}, K_7 \stackrel{\text{def}}{=} \frac{d}{J}, K_8 \stackrel{\text{def}}{=} \frac{1}{J}, \sigma \stackrel{\text{def}}{=} 1 - \frac{M^2}{L_s L_r}, T_r \stackrel{\text{def}}{=} \frac{L_r}{R_r}, m \stackrel{\text{def}}{=} \frac{1}{\sigma L_s}. R_r$ and R_s are the resistances, M is the mutual inductance between the stator and rotor windings, L_s and L_r are respectively, the stator and rotor self-inductances, p is the number of pole-pairs, J is the coefficient of inertia and d is the coefficient of viscous damping.

Remark 1: $\zeta \in \mathbb{R}^6$ is the state, $u \in \mathbb{R}^2$ is the control input, $y \in \mathbb{R}^2$ is the output, and $\ell \in \mathbb{R}^2$ is the measurement noise, $f : \mathbb{R}^6 \to \mathbb{R}^6$ are C^∞ vector fields, and $h : \mathbb{R}^6 \to \mathbb{R}^2$ is a C^∞ functions vector, $f(\zeta, u)$ is the field of nonlinear function, $h(\zeta)$ is the output function, $\dot{\zeta}$ is the derivative of state.

In the sequel, the dynamic of the load torque is modeled as piecewise function:

$$\dot{T}_l = 0 \tag{2}$$

The objective is to determine the states of the motor; $i_{s\alpha}, i_{s\beta}, \phi_{r\alpha}, \phi_{r\beta}, \Omega$, and T_l. This is derived from the input and output, i.e. the voltages $v_{s\alpha}, v_{s\beta}$, and currents $i_{s\alpha}$ and $i_{s\beta}$, measurements. Therefore, the observability of system (1) is studied by considering $y = \{i_{s\alpha}, i_{s\beta}\}$ as an output. For further clarification, the following notations are used:

$$\zeta = \begin{pmatrix} \zeta^1 \\ \zeta^2 \end{pmatrix} \quad \text{with} \quad \zeta^1 = \begin{pmatrix} \zeta_1^1 \\ \zeta_2^1 \\ \zeta_3^1 \end{pmatrix}, \quad \zeta^2 = \begin{pmatrix} \zeta_1^2 \\ \zeta_2^2 \\ \zeta_3^2 \end{pmatrix} \tag{3}$$

where

$$\zeta_1^1 \equiv i_{s\alpha}, \zeta_2^1 \equiv \phi_{r\alpha}, \zeta_3^1 \equiv \phi_{r\beta}, \zeta_1^2 \equiv i_{s\beta}, \zeta_2^2 \equiv \Omega, \zeta_3^2 = T_l$$

Notations I_k and 0_k are used to denote, the $k \times k$ identity and the $k \times k$ null matrices, respectively, and the rectangular $k \times m$ null matrix is denoted by $0_{k \times m}$.

To make the main concept of the items developed in the following sections more understandable, a description of the changes in the coordinates in motor modeling and in the design of the proposed observer is illustrated in Fig. 1.
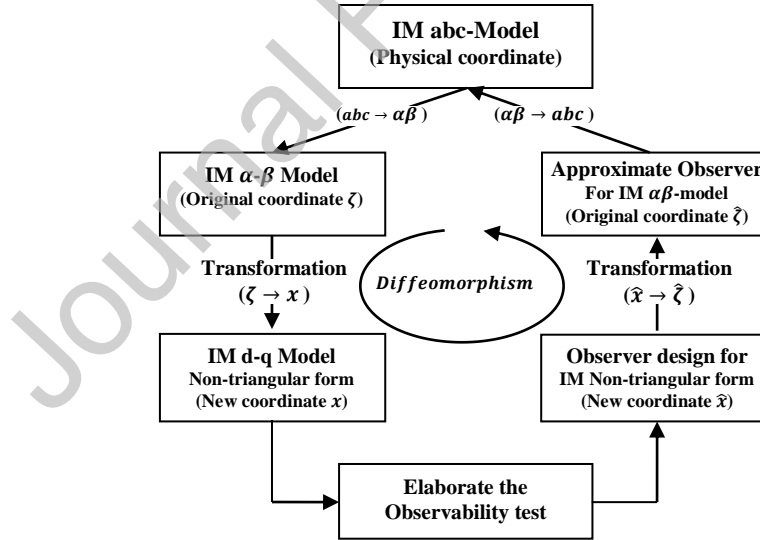
Fig. 1. Illustration describing the proposed methodology.

IM Observability Analysis

As shown in Fig. 1, to design the proposed observer for sensor-less speed estimation of the IM, it is obligatory to analyze the observability property of the IM by using the stator currents and their Lie derivatives [50]. The stator currents equations also read as:

$$\begin{bmatrix} i_{s\alpha} \\ i_{s\beta} \end{bmatrix} = \begin{bmatrix} -K_1 i_{s\alpha} + K_2 \phi_{r\alpha} + K_3 \Omega \phi_{r\beta} \\ -K_1 i_{s\beta} - K_3 \Omega \phi_{r\alpha} + K_2 \phi_{r\beta} \end{bmatrix} + \begin{bmatrix} m & 0 \\ 0 & m \end{bmatrix} \begin{bmatrix} v_{s\alpha} \\ v_{s\beta} \end{bmatrix} \tag{4}$$

By indicating

$$u \overset{\text{def}}{=} \begin{bmatrix} v_{s\alpha} \\ v_{s\beta} \end{bmatrix} \qquad h(\zeta) \overset{\text{def}}{=} \begin{bmatrix} h_1 \\ h_2 \end{bmatrix} \overset{\text{def}}{=} \begin{bmatrix} \zeta_1^1 \\ \zeta_1^2 \end{bmatrix} \overset{\text{def}}{=} \begin{bmatrix} i_{s\alpha} \\ i_{s\beta} \end{bmatrix}$$

let:

$$\mathcal{O}(\zeta) = \begin{pmatrix} h_1 \\ h_2 \\ L_f^1(h_1) \\ L_f^2(h_1) \\ L_f^1(h_2) \\ L_f^2(h_2) \end{pmatrix} \tag{5}$$

where, $\mathcal{O}(\zeta)$ denotes the mapping which constitutes the space of observation [51], and $L_f(h)$ denotes the Lie derivative of h along the function f.

The observability can be evaluated from the Jacobian j of $\mathcal{O}(\zeta)$ with respect to the state vector ζ as:

$$j(\zeta) = \frac{\partial \mathcal{O}(\zeta)}{\partial \zeta} = \begin{bmatrix} A_{\mathcal{O}} & B_{\mathcal{O}} \\ H_{\mathcal{O}} & G_{\mathcal{O}} \end{bmatrix} \tag{6}$$

with

$$A_{\mathcal{O}} = \begin{bmatrix} \dfrac{\partial \mathcal{O}_1^1}{\partial \zeta_1^1} & \dfrac{\partial \mathcal{O}_1^1}{\partial \zeta_1^2} \\ \dfrac{\partial \mathcal{O}_1^2}{\partial \zeta_1^1} & \dfrac{\partial \mathcal{O}_1^2}{\partial \zeta_1^2} \end{bmatrix} = I_2 \,, \quad B_{\mathcal{O}} = \begin{bmatrix} \dfrac{\partial \mathcal{O}_1^1}{\partial \zeta_2^1} & \dfrac{\partial \mathcal{O}_1^1}{\partial \zeta_3^1} & \dfrac{\partial \mathcal{O}_1^1}{\partial \zeta_2^2} & \dfrac{\partial \mathcal{O}_1^1}{\partial \zeta_3^2} \\ \dfrac{\partial \mathcal{O}_1^2}{\partial \zeta_2^1} & \dfrac{\partial \mathcal{O}_1^2}{\partial \zeta_3^1} & \dfrac{\partial \mathcal{O}_1^2}{\partial \zeta_2^2} & \dfrac{\partial \mathcal{O}_1^2}{\partial \zeta_3^2} \end{bmatrix} = 0_{2 \times 4} \,,$$

$$H_{\mathcal{O}} = \begin{bmatrix} H_1 & H_2 \\ H_3 & H_4 \\ H_5 & H_6 \\ H_7 & H_8 \end{bmatrix} \mapsto \begin{cases} H_1 = \dfrac{\partial \mathcal{O}_2^1}{\partial \zeta_1^1} = 0 \\ H_2 = \dfrac{\partial \mathcal{O}_2^1}{\partial \zeta_1^2} = 0 \\ H_3 = \dfrac{\partial \mathcal{O}_2^2}{\partial \zeta_1^1} = 0 \\ H_4 = \dfrac{\partial \mathcal{O}_2^2}{\partial \zeta_1^2} = 0 \end{cases} \,, \quad \begin{cases} H_5 = \dfrac{\partial \mathcal{O}_3^1}{\partial \zeta_1^1} = -K_3 K_6 \phi_{r\beta}^2 \\ H_6 = \dfrac{\partial \mathcal{O}_3^1}{\partial \zeta_1^2} = K_3 K_6 \phi_{r\alpha} \phi_{r\beta} + K_3 K_4 \Omega \\ H_7 = \dfrac{\partial \mathcal{O}_3^2}{\partial \zeta_1^1} = K_3 K_6 \phi_{r\alpha} \phi_{r\beta} - K_3 K_4 \Omega \\ H_8 = \dfrac{\partial \mathcal{O}_3^2}{\partial \zeta_1^1} = -K_3 K_6 \phi_{r\alpha}^2 \end{cases}$$

$$G_O = \begin{bmatrix} G_1 & G_2 \\ G_3 & G_4 \end{bmatrix} \mapsto \begin{cases} G_1 = \begin{bmatrix} G_{11} & G_{12} \\ G_{13} & G_{14} \end{bmatrix} \\ G_2 = \begin{bmatrix} G_{21} & G_{22} \\ G_{23} & G_{24} \end{bmatrix} \\ G_3 = \begin{bmatrix} G_{31} & G_{32} \\ G_{33} & G_{34} \end{bmatrix} \\ G_4 = \begin{bmatrix} G_{41} & G_{42} \\ G_{43} & G_{44} \end{bmatrix} \end{cases} \mapsto \begin{cases} G_{11} = \frac{\partial \mathcal{O}_2^1}{\partial \zeta_2^1} = K_2 \\ G_{12} = \frac{\partial \mathcal{O}_2^1}{\partial \zeta_3^1} = K_3 \Omega \\ G_{13} = \frac{\partial \mathcal{O}_2^2}{\partial \zeta_2^1} = -K_3 \Omega \\ G_{14} = \frac{\partial \mathcal{O}_2^2}{\partial \zeta_3^1} = K_2 \end{cases} \text{ and } \begin{cases} G_{21} = \frac{\partial \mathcal{O}_2^1}{\partial \zeta_2^2} = K_3 \phi_{r\beta} \\ G_{22} = \frac{\partial \mathcal{O}_2^1}{\partial \zeta_3^2} = 0 \\ G_{23} = \frac{\partial \mathcal{O}_2^2}{\partial \zeta_2^2} = -K_3 \phi_{r\alpha} \\ G_{24} = \frac{\partial \mathcal{O}_2^2}{\partial \zeta_3^2} = 0 \end{cases}$$

$$\begin{cases} G_{31} = \frac{\partial \mathcal{O}_3^1}{\partial \zeta_2^1} = K_3 K_6 \phi_{r\beta} i_{s\beta} + K_3 p \Omega^2 \\ G_{32} = \frac{\partial \mathcal{O}_3^1}{\partial \zeta_3^1} = -K_3 K_6 \phi_{r\beta} i_{s\alpha} - K_3 K_5 \Omega + K_3 \dot{\Omega} \\ G_{33} = \frac{\partial \mathcal{O}_3^2}{\partial \zeta_2^1} = -K_3 K_6 \phi_{r\alpha} i_{s\beta} + K_3 K_5 \Omega - K_3 \dot{\Omega} \\ G_{34} = \frac{\partial \mathcal{O}_3^2}{\partial \zeta_3^1} = K_3 K_6 \phi_{r\alpha} i_{s\alpha} + K_3 p \Omega^2 \end{cases} \text{ and } \begin{cases} G_{41} = \frac{\partial \mathcal{O}_3^1}{\partial \zeta_2^2} = -K_3 K_7 \phi_{r\beta} + K_3 \dot{\phi}_{r\beta} - K_3 p \Omega \emptyset_{r\alpha} \\ G_{42} = \frac{\partial \mathcal{O}_3^1}{\partial \zeta_3^2} = K_3 K_8 \phi_{r\beta} \\ G_{43} = \frac{\partial \mathcal{O}_3^2}{\partial \zeta_2^2} = K_3 K_7 \phi_{r\alpha} - K_3 \phi_{r\alpha} + K_3 p \Omega \emptyset_{r\beta} \\ G_{44} = \frac{\partial \mathcal{O}_3^2}{\partial \zeta_3^2} = K_3 K_8 \phi_{r\alpha} \end{cases}$$

By calculating the determinant $\mathcal{D}$ of $\dot{\jmath}(\zeta)$, the associated determinant becomes [12]:

$$\begin{aligned} \mathcal{D} = \frac{-K_3^4}{(pJ)^2} \big(&-p(\zeta_1^2)^2 K_5^2 J \zeta_2^2 - p^3 (\zeta_1^2)^2 J (\zeta_2^2)^3 - p(\zeta_3^1)^3 K_5 K_6 \zeta_2^1 J + p(\zeta_3^1)^2 K_5 \zeta_3^2 \\ &+ p(\zeta_3^1)^2 K_5 K_6 \zeta_1^1 J + p(\zeta_3^1)^2 K_5 K_7 \zeta_2^2 J + p^2 (\zeta_2^2)^2 \zeta_1^1 K_5 J M \zeta_1^1 \\ &+ K_5^3 \zeta_3^1 J M \zeta_2^1 - K_5^2 p(\zeta_3^1)^2 J \zeta_2^2 - K_5 p \zeta_3^1 (\zeta_1^2)^2 J K_6 \zeta_2^1 + K_5^3 \zeta_2^1 J M \zeta_1^1 \\ &+ K_5 p(\zeta_1^2)^2 K_7 \zeta_2^2 J + K_5 p \zeta_3^2 (\zeta_1^2)^2 + K_5 p \zeta_1^1 (\zeta_1^2)^3 J K_6 \\ &- p^2 (\zeta_2^2)^2 \zeta_3^1 K_5 J M \zeta_2^1 - p^3 (\zeta_1^1)^2 J (\zeta_2^2)^3 \big) \end{aligned} \qquad (7)$$

Performing the observability analysis of an IM is a cumbersome task because the expression of determinant $\mathcal{D}$ is very complex. Other cases can be found in [12, 52].

Consider that the motor is operated at zero frequency i.e. the rotor flux components, $\phi_{r\alpha}$ and $\phi_{r\beta}$, are constant. In this case, the new expression of determinant $\mathcal{D}_1$ of the matrix $\dot{\jmath}(\zeta)$ is given by:

$$\mathcal{D}_1 = \frac{-2K_3^4}{p} \underbrace{\big((\zeta_2^1)^2 + (\zeta_3^1)^2 \big)}_{\phi_r^2} \underbrace{\big(K_6 \zeta_1^2 \zeta_2^1 - K_6 \zeta_3^1 \zeta_1^1 - K_7 \zeta_2^2 - K_8 \zeta_3^2 \big)}_{\dot{\zeta}_2^2} \qquad (8)$$

By considering the coefficients K_3, K_6, and K_7 as constant and greater than zero, the determinant $\mathcal{D}_1$ is equal to zero when the flux norm is zero, i.e. $\phi_r = 0$ or when the speed of rotor shaft is constant, i.e.,

$$\dot{\zeta}_5 = \dot{\Omega} = 0 \qquad (9)$$

10

Note that when the rotor shaft speed of IM is constant or the flux norm is zero, the local observability of system (1) might not hold. As shown in [12, 13, 52], the system (1) has regions of operation that are neither observable nor detectable. So, the nonexistence of local observability poses a fundamental limitation to the problem of estimating the system (1) states and that poses a problem of singularity as discussed in the following section. To remedy this problem, it is assumed here that the operating conditions are sufficient to ensure uniform observability of the system.

Observer Design for Sensorless control of IM

As presented in Fig. 1, system (1) is modifiable to the non-triangular observable form (10) and the observer design in the *x*-coordinates. The next goal is to overcome two challenges when implementing the corresponding observer:

1. The use of the observer in the *x*-coordinates cannot be either designed or implemented, because the inverse state transformation needs further reorganization and computation;

2. The use of the corresponding observer in the ζ-coordinates involves the inverse of the matrix of observability (6) that may be ill-conditioned and poses a problem of singularity as discussed in Section 3.

4.1 **Transformation to non-triangular observable form**

The state transformation that allows system (1) to be diffeomorphic to a non-triangular observable canonical form, (13) below, is given in this Section. The transformation of the corresponding system (1) to the non-triangular observable structure is done via the following modification of state coordinates. For the k-th subsystem:

$$x^k = \Phi^k(\zeta) = \begin{bmatrix} h_k(\zeta) & ... & L_f^{\lambda_k - 1} h_k(\zeta) \end{bmatrix}^T \qquad (10)$$

where λ_k are observability indices [53]. Local observability ensures that (11) locally defines *x*-coordinates, i.e., $\Phi(\zeta)$ is a local diffeomorphism.

$$x = \Phi(\zeta) = \begin{bmatrix} \left(\Phi^1(\zeta)\right)^T & ,..., & \left(\Phi^p(\zeta)\right)^T \end{bmatrix}^T \qquad (11)$$

For more detail about the observability and observable forms, the reader is referred to [50, 53-56].

For system (1) with its outputs $h_1 = i_{s\alpha}$ and $h_2 = i_{s\beta}$, and taking the observability indices as $(\lambda_1, \lambda_2) = (3, 3)$, Theorem 1 below, initially proposed in [57] and reformulated in [32], gives a simple proof to verify that the change of state coordinates, given by:

$$x = \Phi(\zeta) = \begin{bmatrix} h_1 & L_f^1(h_1) & L_f^2(h_1) & h_2 & L_f^1(h_2) & L_f^2(h_2) \end{bmatrix}^T \tag{12}$$

transforms system (1) to the non-triangular observable form (13),

$$\begin{aligned} \dot{x} &= Ax + \varphi(x, u) \\ y &= Cx + \ell \end{aligned} \tag{13}$$

where x, u, y and $\varphi(x, u)$ denote the states.

One confirms that the mapping $\Phi(\zeta)$ is the same as $\mathcal{O}(\zeta)$ [50].

Theorem 1 [58] : If the system (1) is observable for any input, then there exists an open dense subset $\mathcal{M}$ of $\mathbb{R}^n$ s.t. for every $x^0 \in \mathcal{M}$, and there exists a neighborhood V, such that the map Φ becomes a diffeomorphism of V in its range. Furthermore, it transforms system (1) restricted to V in canonical form (*x*-coordinates) as (13).

- The output of the new system is expressed as:

$$y = \begin{bmatrix} y_1 \\ y_2 \\ \vdots \\ y_q \end{bmatrix} \in \mathbb{R}^p \tag{14}$$

where, the state $y_k \in \mathbb{R}^{p_k}$, for $k = 1, \dots, q$ and hence $\sum_{k=1}^q p_k = p$

For system (1) with two outputs $h_1 = i_{s\alpha}$ and $h_2 = i_{s\beta}$, the index $k = 2$, and the output of the new system is written as:

$$y = \begin{bmatrix} y_1 \\ y_2 \end{bmatrix} \tag{15}$$

- The state of the new system is given as:

$$x = \begin{bmatrix} x^1 \\ x^2 \\ \vdots \\ x^q \end{bmatrix} \in \mathbb{R}^n \text{ with } x^k = \begin{bmatrix} x_1^k \\ x_2^k \\ \vdots \\ x_{\lambda_k}^k \end{bmatrix} \in \mathbb{R}^{n_k} \tag{16}$$

Remark 2: The variable x^k indicates that the state of the kth subsystem is related with the kth output y^k.

Dimensions of the subsystems are λ_k, $1 \leq k \leq p$, and have $\sum_{k=1}^{q} n_k = \sum_{k=1}^{q} p_k \lambda_k = n$ with $p_k \geq 1$ and $\lambda_k \geq 2$ [43].

For system (1), the number of outputs $q = 2$, and the observability indices are taken as $(\lambda_1, \lambda_2) = (3, 3)$. So, the state of the new system is expressed as:

$$x = \begin{bmatrix} x^1 \\ x^2 \end{bmatrix} \text{ with } x^1 = \begin{bmatrix} x_1^1 \\ x_2^1 \\ x_3^1 \end{bmatrix} \text{ and } x^2 = \begin{bmatrix} x_1^2 \\ x_2^2 \\ x_3^2 \end{bmatrix} \tag{17}$$

- The matrices A and C are set by:

$$A = \text{diag}[A_1 \quad A_2 \quad \cdots \quad A_q], \text{ with } A_k = \begin{bmatrix} 0 & I_{p_k} & \cdot & 0 \\ \vdots & & \ddots & \cdot \\ 0 & \cdots & 0 & I_{p_k} \\ 0 & \cdots & 0 & 0 \end{bmatrix} \in \mathbb{R}^{n_k \times n_k} \tag{18}$$

and

$$C = \text{diag}[C_1 \quad C_2 \quad \cdots \quad C_q], \text{with } C_k = [1 \quad 0] \in \mathbb{R}^{n_k} \tag{19}$$

For system (1), with $q = 2$, $k = 2$ and $p_k = 1$, the matrices A and C are taken as:

$$A = \text{diag}[A_1 \quad A_2], \text{ with } \quad A_1 = A_2 = \begin{bmatrix} 0 & 1 & 0 \\ 0 & 0 & 1 \\ 0 & 0 & 0 \end{bmatrix} \tag{20}$$

and

$$C = \text{diag}[C_1 \quad C_2], \text{ with } \quad C_1 = C_2 = [1 \quad 0 \quad 0] \tag{21}$$

- The field of nonlinear function of the new system is composed as:

$$x = \begin{bmatrix} x^1 \\ x^2 \\ \vdots \\ x^q \end{bmatrix} \in \mathbb{R}^n \text{ with } \varphi^k = \begin{bmatrix} \varphi_1^k \\ \varphi_2^k \\ \vdots \\ \varphi_{\lambda_k}^k \end{bmatrix} \in \mathbb{R}^{n_k} \tag{22}$$

For the given system (1), the nonlinear function field of the new system is expressed as:

$$\varphi(u, x) = \begin{pmatrix} \varphi^1(u, x) \\ \varphi^2(u, x) \end{pmatrix} \tag{23}$$

Given (12), the system in new coordinates considering the change of variables is as below:

$$\boldsymbol{\Phi}: \ \mathbb{R}^6 \to \mathbb{R}^6, \ \ \zeta \to x = \begin{pmatrix} x^1 \\ x^2 \end{pmatrix} = \ \boldsymbol{\Phi}(\zeta) = \begin{pmatrix} \boldsymbol{\Phi}^1(\zeta) \\ \boldsymbol{\Phi}^2(\zeta) \end{pmatrix}$$

where

$$\boldsymbol{\Phi}^1(\zeta) = \begin{pmatrix} \boldsymbol{\Phi}_1^1(\zeta) \\ \boldsymbol{\Phi}_2^1(\zeta) \\ \boldsymbol{\Phi}_3^1(\zeta) \end{pmatrix} = \begin{pmatrix} x_1^1 \\ x_2^1 \\ x_3^1 \end{pmatrix} \text{ and } \boldsymbol{\Phi}^2(\zeta) = \begin{pmatrix} \boldsymbol{\Phi}_1^2(\zeta) \\ \boldsymbol{\Phi}_2^2(\zeta) \\ \boldsymbol{\Phi}_3^2(\zeta) \end{pmatrix} = \begin{pmatrix} x_1^2 \\ x_2^2 \\ x_3^2 \end{pmatrix}$$

and the $\boldsymbol{\Phi}^{k\prime}s$, are defined as below:

$$\begin{cases} \begin{pmatrix} x_1^1 \\ x_2^1 \\ x_3^1 \end{pmatrix} = \begin{pmatrix} h_1 \\ L_f^1(h_1) + g_{u1}(h_1) \\ L_f^2(h_1) + L_f^1(g_{f1}) \end{pmatrix} = \begin{pmatrix} i_{s\alpha} \\ K_2\phi_{r\alpha} + K_3\Omega\phi_{r\beta} \\ K_3\dot{\Omega}\phi_{r\beta} + K_3\Omega\dot{\phi}_{r\beta} \end{pmatrix} \\ \begin{pmatrix} x_1^2 \\ x_2^2 \\ x_3^2 \end{pmatrix} = \begin{pmatrix} h_2 \\ L_f^1(h_2) + g_{u2}(h_2) \\ L_f^2(h_2) + L_f^1(g_{f2}) \end{pmatrix} = \begin{pmatrix} i_{s\beta} \\ K_2\phi_{r\beta} - K_3\Omega\phi_{r\alpha} \\ -K_3\dot{\Omega}\phi_{r\alpha} - K_3\Omega\dot{\phi}_{r\alpha} \end{pmatrix} \end{cases} \quad (24)$$

with

$$g_u(h) = \begin{pmatrix} g_{u1}(h_1) \\ g_{u2}(h_2) \end{pmatrix} = \begin{pmatrix} K_1 i_{s\alpha} - m v_{s\alpha} \\ K_1 i_{s\beta} - m v_{s\beta} \end{pmatrix}; \ g_r = \begin{pmatrix} g_{r\alpha} \\ g_{r\beta} \end{pmatrix} = \begin{pmatrix} K_2\phi_{r\alpha} \\ K_2\phi_{r\beta} \end{pmatrix}; \ g_f = \begin{pmatrix} g_{f1} \\ g_{f2} \end{pmatrix} = g_u(h) - g_r$$

Note that, with the above transformation of state, system (1) gets the non-triangular form (13),

with

$$\varphi^1(u, x) = \begin{pmatrix} \varphi_1^1(u, x) \\ \varphi_2^1(u, x) \\ \varphi_3^1(u, x) \end{pmatrix} = \begin{pmatrix} -g_{u1}(h_1) \\ -L_f^1(g_{r\alpha}) \\ L_f^1[L_f^2(x_1^1) + L_f^1(g_{f1})] \end{pmatrix}$$

and

$$\varphi^2(u, x) = \begin{pmatrix} \varphi_1^2(u, x) \\ \varphi_2^2(u, x) \\ \varphi_3^2(u, x) \end{pmatrix} = \begin{pmatrix} -g_{u2}(h_2) \\ -L_f^1(g_{r\beta}) \\ L_f^1[L_f^2(x_1^2) + L_f^1(g_{f2})] \end{pmatrix}$$

Finally,

$$\begin{cases} \dot{x}_1^1 = x_2^1 - g_{u1}(h_1) \\ \dot{x}_2^1 = x_3^1 - L_f^1(g_{r\alpha}) \\ \dot{x}_3^1 = L_f^1\left(L_f^2(x_1^1) + L_f^1(g_{f1})\right) \\ \dot{x}_1^2 = x_2^2 - g_{u2}(h_2) \\ \dot{x}_2^2 = x_3^2 - L_f^1(g_{r\beta}) \\ \dot{x}_3^2 = L_f^1\left(L_f^2(x_1^2) + L_f^1(g_{f2})\right) \end{cases} \tag{25}$$

Evidently, φ_1^1, φ_2^1 and φ_1^2 and φ_2^2 assure the triangular condition as:

$$\text{For } 1 \leq i \leq \lambda_k - 1 \implies \varphi_i^k(x, u) = \varphi_i^k\left(x^1, x^2, \dots, x^{k-1}, x_1^k, x_2^k, \dots, x_i^k, x_1^{k+1}, x_1^{k+2}, \dots, x_1^q, u\right) \tag{26}$$

The other two components φ_3^1 and φ_3^2, still complicated, are allowed to have dependence on x. Therefore, it can be verified that the system in coordinates (12) is in the non-triangular form.

Remark 3 [26, 59]: To make sure that the system (1) is transformable into (13) is challenging. To solve $x = \Phi(\zeta)$ and its inverse is a difficult task (generally impossible).

4.2 **Notations and definitions for observer design**

In the sequel, some notations and definitions shall be used in the proposed observer equations that will be needed in the convergence analysis of the observation error [43].

Let $\theta: \mathbb{R} \to \mathbb{R}, t \mapsto \theta(t)$ be a real-valued function and for $k = 1, \dots, q$, let $\Delta_k(\theta(t))$, be the diagonal matrix, given as:

$$\Delta_k(\theta(t)) = \text{diag}\left(\frac{I_{p_k}}{\theta(t)^{\delta_k}}, \frac{I_{p_k}}{\theta(t)^{2\delta_k}}, \dots, \frac{I_{p_k}}{\theta(t)^{\lambda_k\delta_k}}\right) \tag{27}$$

where the sequence δ_k, denoting the power of $\theta(t)$, is given by:

$$\begin{cases} \delta_k = 2^{q-k}\left(\prod_{i=k+1}^{q}\left(\lambda_i - \frac{3}{2}\right)\right) \text{ for } k = 1, \dots, q-1 \\ \delta_q = 1. \end{cases} \tag{28}$$

Note that for all $k = 1, \dots, q - 1$, we have:

$$\frac{\delta_k}{2} = \left(\lambda_{k+1} - \frac{3}{2}\right)\delta_{k+1} \tag{29}$$

For $\lambda_k \geq 2 \implies \delta_1 \geq \delta_2 \geq \cdots \geq \delta_q = 1$.

Remark 4 : Due to the interconnection of the subsystems between the block nonlinearities, one has to consider δ_k which are the powers of θ. This idea in fact extends an earlier work where the parameter θ is constant. This result shows a fundamental interest for the next convergence analysis of observation errors. For more information about the proposed high gain hierarchy, refer to [43, 48] .

Lemma 1: For $k, l = 1, \ldots, q$ and $i = 1, \ldots, \lambda_k, j = 2, \ldots, \lambda_l$, let

$$\chi_{l,j}^{k,i} = \begin{cases} 0 & if \ \dfrac{\partial \varphi_i^k}{\partial x_j^i}(x,u) \equiv 0 \\ 1 & othewise \end{cases} \tag{30}$$

and consider the following real sequence:

$$\sigma_i^k = \sigma_1^k + i\delta_k \text{ for } k = 1, \ldots, q \text{ and } i = 1, \ldots, \lambda_k \tag{31}$$

where

$$\sigma_1^k = -\lambda_k \delta_k + \lambda_1 \delta_1 + \left(1 - \frac{1}{2^k}\right) \tag{32}$$

and where the given sequence δ_k's by (28). Then, the terms of this sequence satisfy the following property:

$$if \ \chi_{l,j}^{k,i} = 1 \text{ then } \sigma_j^l - \sigma_i^k - \frac{\delta_k}{2} - \frac{\delta_l}{2} \le -\frac{1}{2^q}. \tag{33}$$

Detailed proof of this Lemma is given in [48]. Yet, two properties of real σ shall be used during this article, namely:

$\mathcal{P}1.$ $For \ k = 1, \ldots, q \ and \ i = 1, \ldots, \lambda_k \ \Rightarrow \ \sigma_i^k > 0$

and

$\mathcal{P}2.$ $For \ k = 1, \ldots, q \ \Rightarrow \ \sigma_{\lambda_k}^k = \sigma_{\lambda_1}^1 + \left(\frac{1}{2} - \frac{1}{2^k}\right).$

As for $\Delta_k{}'s$, one has for $k = 1, \ldots, q$ the diagonal matrices $\Lambda_k{}'s$ as:

$$\Lambda_k(\theta) = \theta^{-\sigma_1^k} \Delta_k(\theta) \tag{34}$$

where $\sigma_1^{k'}s$ are the positive reals specified by Lemma 1 and $\Delta_k(\theta)$ is defined by (27). By considering the structure of matrix relations (18) and (19), one can show that the next identities are:

$$\Lambda_k(\theta) A_k \Lambda_k^{-1}(\theta) = \Delta_k(\theta) A_k \Delta_k^{-1}(\theta) = \theta^{\delta_k} A_k \tag{35}$$

$$C_k \Lambda_k^{-1}(\boldsymbol{\theta}) = \boldsymbol{\theta}^{\sigma_1^k + \delta_k} C_k$$

Also, one can check the following relation:

$$\dot{\Lambda}_k(\boldsymbol{\theta}) \triangleq \frac{d}{dt}\Lambda_k(\boldsymbol{\theta}) = -\frac{\dot{\theta}(t)}{\theta(t)}(\sigma_1^k I_k + \delta_k D_k)\Lambda_k(\boldsymbol{\theta}) \tag{36}$$

where,

I_k: is the identity matrix $k \times k$;

D_k: is the diagonal matrix $n_k \times n_k$, defined as : $D_k = diag(1, 2, \ldots, n_k)$

Moreover, for $k = 1, \ldots, q$, let,

$$\widetilde{K}_k = \begin{bmatrix} \widetilde{K}_{k,1} & \widetilde{K}_{k,2} & \ldots & \widetilde{K}_{k,n_k} \end{bmatrix}^T \tag{37}$$

where $\widetilde{K}_{k,i} \in \mathbb{R}^{p_k \times p_k}$

be the $n_k \times p_k$ matrix such that $\widetilde{A}_k \overset{\text{def}}{=} A_k - \widetilde{K}_k C_k$ is Hurwitz. Then, for a positive real number $a > 0$ and symmetric positive definite $n_k \times n_k$ matrices S_k [43, 60, 61]:

$$\widetilde{A}_k^T S_k + S_k \widetilde{A}_k \leq -a S_k \text{ and } D_k S_k + S_k D_k \geq 0 \tag{38}$$

Based on this relation, one defines certain matrices that shall be used during the convergence analysis of the observation errors, namely:

$$\begin{aligned} Q_k &= S_k D_k + D_k S_k \\ \widetilde{\Omega}_k &= \delta_k Q_k + 2\sigma_1^k S_k \end{aligned} \tag{39}$$

with

$$\begin{aligned} \widetilde{\Omega} &= \text{diag}(\widetilde{\Omega}_1, \widetilde{\Omega}_2, \ldots, \widetilde{\Omega}_q) \\ S &= \text{diag}(S_1, S_2, \ldots, S_q) \end{aligned} \tag{40}$$

and

$$Q_k = Q_k^T \geq 0, \quad \sigma_1^k > 0 \text{ and } S_k = S_k^T > 0$$

4.3 Observer design in x-coordinates

In this section, the observer design is developed for the k-th subsystem and the corresponding system (13), respectively. As defined above, system (1) is developed in the non-triangular observable form (13)

17

that is observable for any input and the designed observer is used to estimate x. Later, Subsection 4.4, estimate of ζ, denoted by $\hat{\zeta}$, is reconstructed from $\hat{x}$.

Assumptions 1: To design the proposed observer, two assumptions are considered:

1. The new system non-linear function, $\varphi(u, x)$, is globally Lipschitz in nature with respect to x uniformly in u.

2. The persistence of input is correlated to the observability of the new system (13).

Observer design for the k-th subsystem

The adaptive non-linear high gain observer design in x-coordinates for k-th subsystem (13) is given by:

$$O_k \begin{cases} \dot{\hat{x}}^k(t) = A_k \hat{x}^k(t) + \varphi^k\big(u(t), \hat{x}(t)\big) - \Delta_k^{-1}\big(\theta(t)\big)\widetilde{K}_k C_k e^k(t) \\ \dot{\theta}(t) = -\frac{1}{2}\mu_1\,\theta(t)\big(a(\theta(t) - 1) - g(t)\gamma(\|\widetilde{y}(t)\|)\big) \text{ with } \theta(0) \geq 1 \\ g(t) = \dfrac{M}{1 + \min(\rho, \mathcal{P}_T(t))} \text{ with } \mathcal{P}_T(t) = \dfrac{1}{T}\int\limits_{\max(0, t-T)}^{t} \|\widetilde{y}(\tau)\|^2 d\tau \end{cases} \quad (41)$$

where $\hat{x} \in \mathbb{R}^n$ indicates the state estimates, defined by:

$$\hat{x} = \begin{bmatrix} \hat{x}^1 \\ \hat{x}^i \\ \vdots \\ \hat{x}^q \end{bmatrix} \in \mathbb{R}^n \text{ with } \hat{x}^k = \begin{bmatrix} \hat{x}_1^k \\ \hat{x}_2^k \\ \vdots \\ x_{\lambda_k}^k \end{bmatrix} \in \mathbb{R}^{n_k}$$

$\hat{x}_i^k \in \mathbb{R}^{p_k}$ indicates a state estimate up to an injection of output for $i = 1, \dots, \lambda_k$ and $k = 1, \dots, q$;

$e^k \in \mathbb{R}^{n_k}$ is the error k-th subcomponent of observation, defined as $e^k = \hat{x}^k - x^k$;

$\widetilde{y} \in \mathbb{R}^p$ is the error k-th subcomponent of output observation, defined as $\widetilde{y} = C(\hat{x} - x)$.

Observer design for the corresponding system

Given the observer structure (41), an observer can be easily designed for system (13), one has

$$q = 2, k = \{1, 2\}, \lambda_1 = \lambda_2 = 3, p_1 = p_2 = 1$$

and has design parameters :

$$\theta(t) \geq 1, \quad \delta_1 = 3; \quad \delta_2 = 1$$

18

$$\Delta_1\big(\theta(t)\big) = diag\left[\frac{1}{\theta^3},\frac{1}{\theta^6},\frac{1}{\theta^9}\right] \quad \Delta_2\big(\theta(t)\big) = diag\left[\frac{1}{\theta},\frac{1}{\theta^2},\frac{1}{\theta^3}\right]$$

$$\widetilde{K}_1 = S_1^{-1}C_1^T = [3,3,1], \qquad \widetilde{K}_2 = S_2^{-1}C_2^T = [3,3,1].$$

By replacing these design parameters with the k-th subsystem (41), the observer can be obtained in x-coordinates as below:

$$
\begin{aligned}
O_1 &\begin{cases} \dot{\hat{x}}^1(t) = A_1\hat{x}^1(t) + \varphi^1\big(u(t),\hat{x}(t)\big) - \Delta_1^{-1}\big(\theta(t)\big)\widetilde{K}_1C_1e^1(t) \\ \hat{y}_1 = C_1\hat{x}^1 \end{cases} \\
O_2 &\begin{cases} \dot{\hat{x}}^2(t) = A_2\hat{x}^2(t) + \varphi^2\big(u(t),\hat{x}(t)\big) - \Delta_2^{-1}\big(\theta(t)\big)\widetilde{K}_2C_2e^2(t) \\ \hat{y}_1 = C_1\hat{x}^1 \end{cases}
\end{aligned} \tag{42}
$$

The Riccati differential equation that governs the dynamics of the gain parameter $\theta(t)$ is similar to that given in (41).

Remark 5 [43]: Equations of the observer are required to specify three design parameters M, T and ρ jointly with the function $\gamma(\|\tilde{y}(t)\|)$, and $\mu_1 = \frac{\lambda_m(S)}{\lambda_M(\widetilde{\Omega})}$, where $\lambda_m(S)$ and $\lambda_M(\widetilde{\Omega})$ are the smallest and the largest eigenvalues, respectively, $\widetilde{\Omega}$ and S are defined by (40) and, finally $\gamma(\|\tilde{y}(t)\|) = \frac{\|\tilde{y}(t)\|^2}{1+\|\tilde{y}(t)\|^2}$.

Theorem 2 [43]**:** Under Assumption 1 and for high values of the parameter M, the trajectories of the proposed observer (41) converge exponentially to those of system (13).

4.4 **Observer design in ζ-coordinates**

Without the inverse state transformation of the closed-form $\zeta = \Phi^{-1}(x)$, the nonlinear function of $\varphi\big(u(t),\hat{x}(t)\big)$ cannot be obtained as discussed above. To implement the observer in the x-coordinates (41), further rearrangement such as, rewriting $\varphi\big(\hat{x}(t),u(t)\big)$ as a function of $\big(\Phi(\zeta),u(t)\big)$, is needed. In this case, the x-observer is adjusted as:

$$
O_k \begin{cases} \dot{\hat{x}}^k(t) = A_k\hat{x}^k(t) + \varphi^k\big(\phi(\hat{\zeta}),u(t)\big) - \Delta_k^{-1}\big(\theta(t)\big)\widetilde{K}_kC_ke^k(t) \\ \hat{y}_k = C_k\hat{x}^k \end{cases} \tag{43}
$$

where $\varphi^k\big(\Phi(\hat{\zeta}),u(t)\big)$ are the rows corresponding to the k-th subsystem in $\varphi\big(\Phi(\hat{\zeta}),u(t)\big)$ given by:

$$\varphi\big(\Phi(\hat{\zeta}),u(t)\big) = \frac{\partial\Phi(\hat{\zeta})}{\partial\hat{\zeta}}\big(f(\hat{\zeta},u)\big) - A\,\Phi(\hat{\zeta})$$

Consequently, the observer (43) can be implemented as:

$$O_k \begin{cases} \dot{\hat{x}}^k(t) = \dfrac{\partial \Phi^k(\hat{\zeta})}{\partial \hat{\zeta}} \left(f^k(\hat{\zeta}, u) \right)_k - \Delta_k^{-1}(\theta(t)) \widetilde{K}_k C_k e^k(t) \\ \hat{y}_k = C_k \hat{x}^k \end{cases} \tag{44}$$

where $\hat{\zeta}$ is numerically constructed by resolving n nonlinear algebraic equations (12).

Remark 6 :

- If $\dfrac{\partial \Phi^k(\hat{\zeta})}{\partial \hat{\zeta}^k}$ is singular, the *x*- coordinates may not be well defined and the observer is invalid.

- Even if the *x*-coordinates are well-defined, $\Phi^k(\hat{\zeta})$ is non-convex, indicating that (12) might have multiple solutions.

If the transformation of state, $\Phi^k(\hat{\zeta})$, is a local diffeomorphism in the neighborhood of ζ_0, its Jacobian $\dfrac{\partial \Phi^k(\hat{\zeta})}{\partial \hat{\zeta}^k}$ in the neighborhood is non-singular. As shown in Fig. 1, the observer (42) can be implemented as;

$$O_k \begin{cases} \dot{\hat{\zeta}}^k(t) = f(\hat{\zeta}^k, u) - \left(\dfrac{\partial \Phi^k(\hat{\zeta})}{\partial \hat{\zeta}^k} \right)^{-1} \Delta_k^{-1}(\theta(t)) \widetilde{K}_k C_k e^k(t) \\ \hat{y}_k = C_k \hat{x}^k = h(\hat{\zeta}^k) \end{cases} \tag{45}$$

Note that,

$$\left(\frac{\partial \Phi^k(\hat{\zeta})}{\partial \hat{\zeta}^k} \right)^{-1} \equiv j(\zeta)^{-1}$$

Observer (45) results in a lower computation cost than observer (44), although it also can suffer from mistaken state estimation.

4.5 Approximate Observer Design

Implementation of the observer (45) requires that the inverse of the observability matrix $\left(\dfrac{\partial \Phi^k(\hat{\zeta})}{\partial \hat{\zeta}^k} \right)^{-1}$ be solved in real-time. However, implementation problems hinder the observer's efficiency as it requires the inversion of the Jacobian matrix. Since the induction motor can operate in its unobservable region, the Jacobian is regular almost everywhere. To remedy this, an appropriate implementation procedure based on two approximations of the inverse Jacobian matrix, from (6), we have:

$$j(\zeta)^{-1} = \begin{bmatrix} I_2 & 0_{2\times4} \\ G_O^{-1}H_O & G_O^{-1} \end{bmatrix} \tag{46}$$

The structure of (46), based on the first approximation is governed by the consideration of reducing complexity without requiring the observer convergence. The motivation for second approximation is safety computational considerations without requiring observer efficiency [20].

Decomposition of the Jacobian matrix inverse based on the simplicity oriented approximation is given as:

$$j(\zeta)^{-1} = \Lambda_L + \Lambda_U \tag{47}$$

where

$$\Lambda_L = \begin{bmatrix} 0_2 & 0_{2\times4} \\ -G_O^{-1}H_O & 0_{4\times4} \end{bmatrix}; \quad \Lambda_U = \begin{bmatrix} I_2 & 0_{2\times4} \\ 0_{4\times2} & G_O^{-1} \end{bmatrix}$$

This leads to the low triangular matrix with zeros on the diagonal as:

$$\Gamma(\zeta) \triangleq j(\zeta)\Lambda_L = \begin{bmatrix} 0_2 & 0_{2\times4} \\ -G_O G_O^{-1}H_O & 0_{4\times4} \end{bmatrix} \tag{48}$$

Matrix Λ_U is an adequate approximation of the inverse of Jacobian matrix in the sense that it does not question the proposed observer accuracy as in [8, 10]. However, such an approximation remains questionable from the efficiency of computation perspective, because the matrix G_O becomes no longer invertible as soon as the trajectory of the state of the observer evolves in the unobservable domain of the IM. To avoid this problem, the observer (45) should be implemented by a judicious approach to the Λ_U matrix.

The approximation of Λ_U is reduced to looking for an approximation of G_O. To this end, consider the following factorization:

$$G_O = L\,U \tag{49}$$

with

$$L = \begin{bmatrix} I_2 & 0_2 \\ G_3 G_1^{-1} & \underbrace{G_4 - G_3 G_1^{-1} G_2}_{L_O} \end{bmatrix}; \quad U = \begin{bmatrix} G_1 & G_2 \\ 0_2 & I_2 \end{bmatrix}$$

It is clear from the structures of L and U, that matrices G_O and L_O have the same singular points. As a result, it is sufficient to look for an approximation for the inverse of L_O to approximate G_O. The inverse

of L_O can be approximated by using a technique called the Tikhonov regulation [49]. It introduces a positive constant δ into the formula of L_O, denoted by L_O^+, given as:

$$L_O^+ = \left(L_O^T L_O + \delta I_2\right)^{-1} L_O^T \quad \text{where} \quad \delta > 0 \tag{50}$$

By introducing an arbitrarily small positive number δ, the Tikhonov regularization reduces the condition number of $L_O^T L_O$ and, therefore, results in an improvement of the resolution accuracy. By following the proposed approximation, the matrix G_O^{-1} is expressed as:

$$G_O^+ = \begin{bmatrix} G_1^{-1} + G_1^{-1} G_2 L_O^+ G_3 G_1^{-1} & -G_1^{-1} G_2 L_O^+ \\ -L_O^+ G_3 G_1^{-1} & L_O^+ \end{bmatrix} \tag{51}$$

Following these two approximations, the inverse of the Jacobian matrix intervening in the equation of the observer (45), noted as Λ_U^+, is computed as:

$$\Lambda_U^+ = \begin{bmatrix} I_2 & 0_{2\times4} \\ 0_{4\times2} & G_O^+ \end{bmatrix} \tag{52}$$

An observer of structure (42) is designed for the IM. Equations of the proposed observer are:

$$O_1 \begin{cases} \begin{pmatrix} \dfrac{d\hat{\imath}_{s\alpha}}{dt} \\ \dfrac{d\hat{\phi}_{r\alpha}}{dt} \\ \dfrac{d\hat{\phi}_{r\beta}}{dt} \end{pmatrix} = \begin{pmatrix} -K_1\hat{\imath}_{s\alpha} + K_2\hat{\phi}_{r\alpha} + K_3\hat{\Omega}\hat{\phi}_{r\beta} \\ K_4\hat{\imath}_{s\alpha} - K_5\hat{\phi}_{r\alpha} - p\hat{\Omega}\hat{\phi}_{r\beta} \\ K_4\hat{\imath}_{s\beta} + p\hat{\Omega}\hat{\phi}_{r\alpha} - K_5\hat{\phi}_{r\beta} \end{pmatrix} + \begin{pmatrix} m & 0 \\ 0 & 0 \\ 0 & 0 \end{pmatrix} \begin{pmatrix} u_{s\alpha} \\ u_{s\beta} \end{pmatrix} \\ \qquad\qquad -\Lambda_{U1}^+(\hat{\zeta}) \begin{pmatrix} 3\theta^3(t) \\ 3\theta^6(t) \\ \theta^9(t) \end{pmatrix} (\hat{\imath}_{s\alpha} - i_{s\alpha}) \\ \hat{y}^1 = \hat{\imath}_{s\alpha} \end{cases} \tag{53}$$

$$O_2 \begin{cases} \begin{pmatrix} \dfrac{d\hat{\imath}_{s\beta}}{dt} \\ \dfrac{d\hat{\Omega}}{dt} \\ \dfrac{d\hat{T}_l}{dt} \end{pmatrix} = \begin{pmatrix} -K_1\hat{\imath}_{s\beta} - K_3\hat{\Omega}\hat{\phi}_{r\alpha} + K_2\hat{\phi}_{r\beta} \\ K_6(\hat{\phi}_{r\alpha}\hat{\imath}_{s\beta} - \hat{\phi}_{r\beta}\hat{\imath}_{s\alpha}) - K_8\hat{T}_l - K_7\hat{\Omega} \\ 0 \end{pmatrix} + \begin{pmatrix} 0 & m \\ 0 & 0 \\ 0 & 0 \end{pmatrix} \begin{pmatrix} u_{s\alpha} \\ u_{s\beta} \end{pmatrix} \\ \qquad\qquad -\Lambda_{U2}^+(\hat{\zeta}) \begin{pmatrix} 3\theta(t) \\ 3\theta^2(t) \\ \theta^3(t) \end{pmatrix} (\hat{\imath}_{s\beta} - i_{s\beta}) \\ \hat{y}^2 = \hat{\imath}_{s\beta} \end{cases} \tag{54}$$

$$\theta(t) \quad \left\{ \dot{\theta}(t) = -\frac{1}{2}\mu_1\,\theta(t)\big(a(\theta(t) - 1) - \mathbf{g}(t)\gamma(\|\widetilde{y}(t)\|)\big) \right. \tag{55}$$

with $\theta(t) \geq 1$, $\mathbf{g}(t) = \frac{M}{1+\min(\rho, \mathcal{P}_T(t))}$, $\mathcal{P}_T(t) = \frac{1}{T}\int_{\max(0,t-T)}^{t}\|\widetilde{y}(\tau)\|^2 d\tau$ and $\Lambda_{U1}^{+}(\hat{\zeta})$ and $\Lambda_{U2}^{+}(\hat{\zeta})$ are,

respectively, calculated from the approximate matrix Λ_U^{+} taking into account the rearrangement of their

rows and columns according to an arrangement of the states of two interconnected observers.

Remark 7: The physical operation domain D of an IM is defined as:

$$D = \big\{ \zeta \in \mathbb{R}^6 \mid |i_{s\alpha}| \leq i_{s\alpha}^{max}, |i_{s\beta}| \leq i_{s\beta}^{max}, |\phi_{r\alpha}| \leq \phi_{r\alpha}^{max}, |\phi_{r\beta}| \leq \phi_{r\beta}^{max}, |\Omega| \leq \Omega^{max}, |T_l| \leq T_l^{max} \big\}$$

where $\zeta = \begin{bmatrix} i_{s\alpha} & i_{s\beta} & \phi_{r\alpha} & \phi_{r\beta} & \Omega & T_l \end{bmatrix}^T$, and $i_{s\alpha}^{max}, i_{s\beta}^{max}, \phi_{r\alpha}^{max}, \phi_{r\beta}^{max}, \Omega^{max}$ and T_l^{max} are the actual

maximum values for stator currents, rotor flux, rotor shaft speed and load torque, respectively. These

maximum values are defined from the motor specification sheet.

Remark 8: Globally exponential stability for the trajectories of system observer for high values of the

parameter **M** are established by Theorem 3 (Theorem 4.1 of [43]).

Theorem 3 [48]: Assume that the given system (1) satisfies assumption (1-a), then

$$\forall M > 0; \ \exists\theta_0 > 0; \ \forall\theta > \theta_0; \ \exists\lambda_\theta > 0; \ \exists\alpha_\theta > 0 \text{ s.t. for } k \in \{1, \dots, q\}$$

$$\big\|\hat{x}^k(t) - x^k(t)\big\| \leq \lambda_\theta e^{-\mu_\theta t}\big\|\hat{x}^k(0) - x^k(0)\big\| \tag{56}$$

for admissible control u with $|u|_\infty \leq M$. Moreover, λ_θ is a polynomial in θ and $lim_{\theta \to \infty} +\infty$.

4.6 **Observer tuning**

As mentioned previously, the standard high-gain observer design techniques based on observable

canonical form reveal that a trade-off exists between the sensitivity of measurement noise and quick

convergence. Moreover, such type of observer faces the so-called "peaking phenomenon" of the internal

states of the observer exhibited during the transient period, which may lead to a destabilization of the

system. To deal with this trade-off, the observer gain, involving the use of a scalar time-varying design

parameter governed by the Riccati differential equation (55), guarantees the best compromise between the

fast convergence of the states and noise rejection. With such an adaptation, the gain parameter of the

observer assume small value during the transient period of the observer internal states and prevent system

peaking.

As shown in equation (55), the latter involves three design parameters M, T and ρ. The choice of the parameter ρ is mainly introduced to saturate the integral term $\frac{1}{T} \int_{\max(0,t-T)}^{t} \|\widetilde{y}(\tau)\|^2 d\tau$.

Recall that the real-valued function $\gamma(\cdot)$ is non-negative, non-decreasing and bounded with $\gamma(0) > 0$ and $\gamma(x) > 0$ for $x > 0$. The function that has been used in the corresponding system in simulation is:

$$\gamma(\|\widetilde{y}(t)\|) = \frac{\|\widetilde{y}(t)\|^2}{1 + \|\widetilde{y}(t)\|^2} \tag{57}$$

where

$$\|\widetilde{y}(t)\| \in \mathbb{R}_+^*.$$

Furthermore, the function $g(t)$ can be written as:

$$g(t) = \frac{M}{1 + \min(\rho, \mathcal{P}_T(t))} \tag{58}$$

and

$$\mathcal{P}_T(t) = \frac{1}{T} \int_{\max(0,t-T)}^{t} \|\widetilde{y}(\tau)\|^2 d\tau$$

The function $\mathcal{P}_T(t)$ represents the power of the output observation error $\widetilde{y}(\tau)$ which is determined on a moving window with a width equal to T. It is, therefore, clear that the function $g(t)$ is bounded as below:

$$\forall\, t \geq 0 : \frac{M}{1 + \rho} \leq g(t) \leq M. \tag{59}$$

Notice that, in the absence of noise measurements, the parameter M can be set to high values. This allows the gain parameter $\theta(t)$ to quickly reach high values. As a result, the observation error vanishes quickly and, therefore, the decrease of the values of the parameter $\theta(t)$ to the predefined value $\theta(t) = 1$ is achieved. However, when the presence of noise measurements is inevitable, the adoption of high values of M should be avoided. Indeed, as mentioned previously, high values of M allow the gain parameter $\theta(t)$ to reach high values and the observer becomes very sensitive to noise. From a noise insensitivity point of view, the value of M is divided by the power of the output observation error that is calculated on a moving window with a width equal to T. It should be noted that small values of T are more advisable in the presence of noise measurements with a variance which continuously varies significantly and relatively

rapidly. On the contrary, in the case where the variance of the noise measurements is constant or varies slowly, the values of T should be relatively high.

Convergence Analysis of The Proposed Observer

In this section, convergence of the proposed observer is analyzed. For that, the boundedness of the design parameter $\theta(t)$ must be proven first by providing expressions of the corresponding lower and upper bounds. The inspiration for the proof comes from the development given in [43].

5.1 *Boundedness of $\theta(t)$*

For this purpose, two cases according to the sign of $\dot{\theta}(t)$ need to be considered. Before that, one notes that the expression of $\dot{\theta}(t)$ in (55) as :

$$\theta = 1 \ \Rightarrow \ \dot{\theta} \geq 0 \tag{60}$$

As a result, as soon as $\theta(0) \geq 1$, one has

$$\forall \, t \geq 0 : \ \theta(t) \geq 1 \tag{61}$$

One also notices that:

$$\forall \, t \geq 0 : 0 < g(t) \leq M. \tag{62}$$

• Case $\dot{\theta}(t) \geq 0$:

Since $\theta(t) \geq 1$ and according to (55), one has $a(\theta(t) - 1) - g(t)\gamma(\|\widetilde{y}(t)\|) \leq 0$ which implies that :

$$\theta(t) \leq 1 + \frac{g(t)\gamma(\|\widetilde{y}(t)\|)}{a} \leq 1 + \frac{M}{a}\gamma(\|\widetilde{y}(t)\|). \tag{63}$$

Thus,

$$\forall \, t \geq 0 : 0 < \theta(t) \leq 1 + \frac{M\gamma_{max}}{a} \tag{64}$$

where γ_{max} is the upper bound of $\gamma(\|\widetilde{y}(t)\|)$.

• Case $\dot{\theta}(t) \leq 0$:

Since $\theta(t) \geq 1$ and from (55), one has:

$$\begin{aligned}
\dot{\theta}(t) \ &\leq \ -\frac{\mu_1}{2}\big(a(\theta(t) - 1) - g(t)\gamma(\|\widetilde{y}(t)\|)\big) \\
&= \ -\frac{a\mu_1}{2}\theta(t) + \frac{a\mu_1}{2}\left(1 + \frac{M\gamma_{max}}{a}\right).
\end{aligned} \tag{65}$$

Integrating (55) from some $t_0 < t$ to t yields:

$$
\begin{aligned}
\theta(t) &\leq e^{-\frac{a\mu_1}{2}(t-t_0)}\theta(t_0) + \left(1 + \frac{M\gamma_{max}}{a}\right) \\
&\leq \theta(t_0) + \left(1 + \frac{M\gamma_{max}}{a}\right).
\end{aligned} \tag{66}
$$

Now, the time t_0 may be either 0, in which case $\theta(0) \geq 1$ is arbitrary, or the final time of an interval on which $\dot{\theta}(t) \geq 0$ and according to (64), one has $\theta(t_0) \leq 1 + \frac{M\gamma_{max}}{a}$. As a result, for any t_0, one has:

$$
\theta(t_0) \leq max\left(\theta(t_0), 1 + \frac{M\gamma_{max}}{a}\right) \tag{67}
$$

Using (67), inequality (66) becomes:

$$
\theta(t) \leq max\left(\theta(t_0), 1 + \frac{M\gamma_{max}}{a}\right) + \left(1 + \frac{M\gamma_{max}}{a}\right) \tag{68}
$$

To summarize and according to (64) and (68), $\theta(t)$ is bounded and satisfies:

$$
\forall t \geq 0 : \theta(t) \leq max\left(\theta(t_0), 1 + \frac{M\gamma_{max}}{a}\right) + \left(1 + \frac{M\gamma_{max}}{a}\right) \tag{69}
$$

5.2 Convergence analysis for x-observer

In this subsection, the convergence analysis for the x-observer is presented, and then the convergence analysis for ζ-observer is deduced.

The time derivative of $e^k(t) = \hat{x}^k(t) - x^k(t)$ is :

$$
\dot{e}^k = A_k e^k + \varphi^k(u, \hat{x}) - \varphi^k(u, x) - \Delta_k^{-1}(\theta)\widetilde{K}_k C_k e^k \tag{70}
$$

where u is an allowable control such that $\| u \|_\infty \leq \eta$, where η is a positive scalar.

For k-th subsystem, $k = 1, ..., q$, let,

$$
\overline{e}^k = \Lambda_k(\theta)e^k \tag{71}
$$

where $\Lambda_k(\theta)$ is given by (34). From (70) and using (35) and (36), one gets the following:

$$
\dot{\overline{e}}^k = \Lambda_k(\theta)\dot{e}^k + \dot{\Lambda}_k(\theta)\Lambda_k^{-1}(\theta)\overline{e}^k \tag{72}
$$

After some calculations, equation (72) is reduced to:

$$
\dot{\overline{e}}^k = \theta^{\delta_k}\widetilde{A}_k\overline{e}^k + \Lambda_k(\theta)\left(\varphi^k(u, \hat{x}) - \varphi^k(u, x)\right) - \frac{\dot{\theta}}{\theta}\left(\sigma_1^k I_k + \delta_k D_k\right)\overline{e}^k \tag{73}
$$

Let the candidate Lyapunov be:

26

$$V(\bar{e}) = \sum_{k=1}^{2} V_k\left(\bar{e}^k(t)\right) = \bar{e}^T S \bar{e} \tag{74}$$

with

$$V_k\left(\bar{e}^k\right) = \bar{e}^{k^T} S_k \bar{e}^k \tag{75}$$

where S is given by (39-40). According to (71) and (75) and from the fact $\sigma_i^k > 0$, for $\theta(t) \geq 1$:

$$\forall\, t \geq 0: \quad \left\|e^k(t)\right\|^2 \leq \left\|\bar{e}^k(t)\right\|^2 \leq \frac{1}{\lambda_m(S_k)} V_k\left(\bar{e}^k(t)\right) \tag{76}$$

which gives:

$$\forall\, t \geq 0: \quad \|e(t)\| \leq \|\bar{e}(t)\| \leq \frac{1}{\sqrt{\lambda_m(S)}} \sqrt{V\left(\bar{e}(t)\right)} \tag{77}$$

After some calculations, $\dot{V}_k$ is derived as:

$$\dot{V}_k = 2\bar{e}^{k^T} S_k \bar{e}^k = 2\theta^{\delta_k}\bar{e}^{k^T} S_k \tilde{A}_k \bar{e}^k + 2\bar{e}^{k^T} S_k \Lambda_k(\theta)\left(\varphi^k(u,\hat{x}) - \varphi^k(u,x)\right) - \frac{\dot{\theta}}{\theta}\bar{e}^{k^T}\tilde{\Omega}_k \bar{e}^k \tag{78}$$

where the SPD matrix $\tilde{\Omega}_k$ is given by (39), and $\sigma_i^k \, and \, \sigma_j^l$ are given in (32). Using (38), and after

some calculation one obtains:

$$\dot{V}_k \leq -a\theta^{\delta_k} V_k + 2\lambda_k \rho_k \mu(S)\theta^{-\frac{1}{2q}}\sqrt{\theta^{\delta_k} V_k} \times \sum_{l=1}^{q}\sum_{j=2}^{\lambda_l}\sqrt{\theta^{\delta_l} V_l} - \frac{\dot{\theta}}{\theta}\bar{e}^{k^T}\tilde{\Omega}_k\bar{e}^k \tag{79}$$

where

$$\rho_k = sup\left\{\left\|\frac{\partial\varphi_i^k}{\partial x_j^l}(u,x)\right\| ; x \in \mathbb{R}^n \, and \, \|u\|_\infty \leq \eta\right\};$$

with $\chi_{l,j}^{k,i\prime}s$ defined in (30), and

$$\theta^{\,\sigma_j^l - \sigma_i^k - \frac{\delta_k}{2} - \frac{\delta_l}{2}} \leq \theta^{-\frac{1}{2q}} \tag{80}$$

Now, setting

$W_k\left(\bar{e}^k\right) = \bar{e}^{k^T}\tilde{\Omega}_k\bar{e}^k \, and \, W(\bar{e}) = \bar{e}^T\tilde{\Omega}\bar{e} = \sum_{k=1}^{q} W_k\left(\bar{e}^k\right)$, one gets:

$$\mu_1 W_k \leq V_k \leq \mu_2 W_k \tag{81}$$

where,

$$\mu_1 \triangleq \frac{\lambda_m(S)}{\lambda_M(\widetilde{\Omega})} \quad, \qquad \mu_2 \triangleq \frac{\lambda_M(S)}{\lambda_m(\widetilde{\Omega})} \quad \text{and} \quad \frac{\mu_2}{\mu_1} = \mu(S)\mu(\widetilde{\Omega})$$

Now, for $k = 1, \ldots, q$, set $V_k^* = a\theta^{\delta_k} V_k$ and let $V^* = \sum_{k=1}^q V_k^*$. Since $\theta \geq 1$, according to (29):

$$a\theta V = a\theta^{\delta_q} V \leq V^* \leq a\theta^{\delta_1} V \tag{82}$$

Then, the inequality (79) becomes:

$$\dot{V}_k \leq -V^* + 2n^2 \frac{\rho}{a} \mu(S) \theta^{-\frac{1}{2q}} V^* - \frac{\dot{\theta}}{\theta} W \tag{83}$$

where,

$$V^* = \sum_{k=1}^2 V_k^* = V_1^* + V_2^*$$

and $\rho = \max\{\rho_k, 1 \leq k \leq q\}$. Substituting $\frac{\dot{\theta}}{\theta}$ by its expression, one has:

$$\dot{V} \leq -V^* + 2n^2 \frac{\rho}{a} \mu(S) \theta^{-\frac{1}{2q}} V^* + \frac{\mu_1}{2} \big(a(\theta - 1) - g(t)\gamma(\|\widetilde{y}(t)\|) \big) W \tag{84}$$

For any $\theta \geq 1$, one has:

$$\dot{V}(t) \leq -\frac{1}{4} a(\theta + 1) V(t) + \frac{a\theta_c^{\delta_1 + \frac{1}{2q}}}{4} V(t) - \frac{\mu_1}{4\mu_2} g(t)\gamma(\|\widetilde{y}(t)\|) V(t). \tag{85}$$

with

$$\theta_c \triangleq \left(8n^2 \frac{\rho}{a} \mu(S) \right)^{2q}$$

The remainder of the proof of the boundedness of $\theta(t)$, the boundedness of the output observation error $\varepsilon(t)$ and the boundedness of the observation error $e(t)$ are successively proven in [35].

5.3 Convergence analysis for ζ-observer

On condition that $\Phi(\zeta)$ is a local diffeomorphism on an open domain, $\mathcal{B}_x$ has a compact domain $\mathcal{D}$ and $\forall x \in \mathcal{D}$, so is its inverse [20]. The convergence of the zero solution for $\widetilde{x}$ also implies the convergence of $\widetilde{\zeta} = \widehat{\zeta} - \zeta$ as:

$$\left\| \hat{\zeta}^k - \zeta^k \right\| = \left\| \Phi^k(\hat{x})^{-1} - \Phi^k(x)^{-1} \right\|$$

$$\leq \left| \frac{\partial \Phi^k(\epsilon)^{-1}}{\partial \epsilon^k} \right|_\infty \left\| \hat{x}^k - x^k \right\|$$

$$\leq \left| \frac{\partial \Phi^k(\epsilon)^{-1}}{\partial \epsilon^k} \right|_\infty \lambda_\theta e^{-\mu_\theta t} \left\| \hat{x}^k(0) - x^k(0) \right\| \tag{86}$$

ϵ^k: is some value between x^k and $\hat{x}^k$. It is from mean-value theorem or Taylor series first order expansion.

$\left| \frac{\partial \Phi^k(\epsilon)^{-1}}{\partial \epsilon^k} \right|_\infty$ is calculated over all $\epsilon^k \in \mathcal{B}_x$.

Simulation Results

To better appreciate the effectiveness of the proposed observer, simulations studies have been carried out according to the observer–controller scheme presented in Fig. 2.
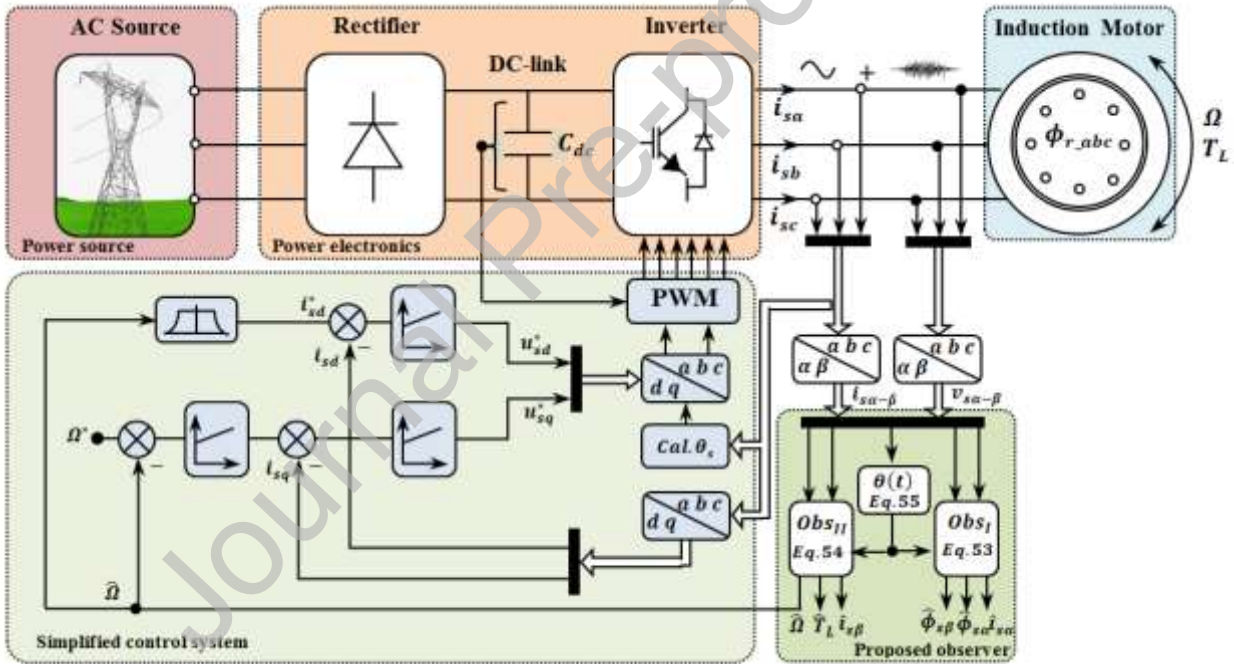
Fig. 2 Basic scheme of observer-controller.

Controller topology shown in Fig. 2 is based on the strategy of Field Oriented Control in order to obtain the same decoupling between flux and torque naturally existing in the DC machines [62]. In this control strategy, the reference rotor angular speed is compared with the feedback signal and the result (error) drives a standard PI controller to determine the quadrature component of the stator current reference to control the electromagnetic torque, while the direct component of the stator current reference

29

is in charge of controlling the magnetic state of the IM. The voltage controls in the d-q reference frame are generated by the two stator current control loop PI controllers.

The proposed observer is tested according to industrial test conditions shown in Fig. 3 [13]. This benchmark is used to validate the proposed observer for sensor-less speed estimation of IM by specifying the operating conditions for the duration of simulation which started at 0 s and ended at 12 s.
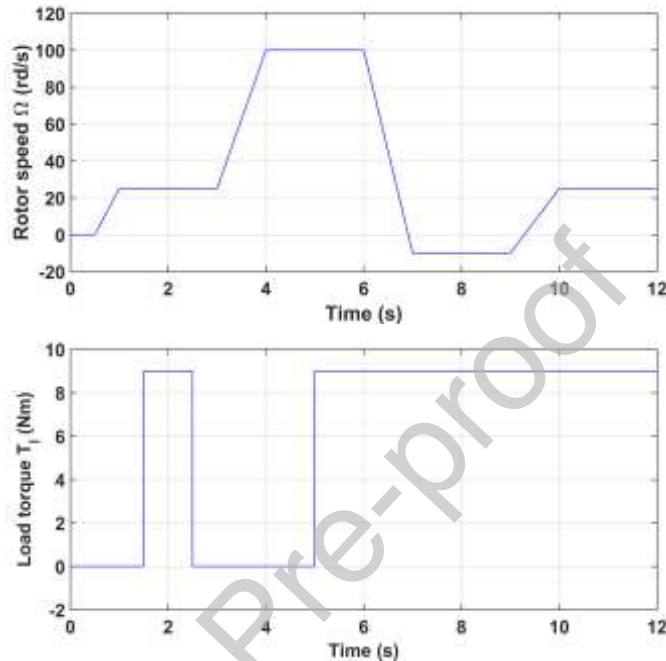
Fig. 3. Industrial benchmark trajectories [13] .

It is proposed to use the industrial benchmark trajectories to verify the IM under an unobservability condition. The rotor shaft speed and the load torque are both zero at initial time. The rotor speed is then increased to 25 rad/s, and a 9 Nm load torque is applied from 1.5 s to 2.5 s. This first step permits the robustness and the performance of the proposed observer to be tested at low rotor speed. The rotor speed, then is increased to 100 rad/s from 3 s to 4 s and remains constant until 6 s with a constant load torque applied from 5 s to 12 s. This second step allows the proposed observer to be tested during a large transient rotor speed and its robustness to be checked at a high speed. Then, the IM is driven at negative speed from 7 s to 9 s at a working torque which keeps the same value.

MATLAB was used to implement the proposed observer for sensor-less speed estimation of the IM. The parameters of the motor are listed in Table I.

TABLE I.   INDUCTION MOTOR PARAMETERS

Parameters	Symbols	Value	Unit
Power	P	1500	W
Rated speed	Ω	1445	tr/mn
Load torque	T_{em}	9	N.m
Power supply voltage	U	380	V
Number of Pole Pairs	p	2	/
Stator resistance	R_s	5.05	Ω
Rotor resistance	R_r	4.06	Ω
Stator inductance	L_s	0.336	H
Rotor inductance	L_r	0.336	H
Mutual	M	0.322	H
Inertia moment	J	0.032	$Kg.m^2$
Viscous friction	f	0.0059	N.m.s/rad

To test the behavior of the proposed observer with respect to noise measurements, two scenarios are simulated: first the measurements of motor states are considered free of noise; then the operating conditions are corrupted by noise produced by a PWM converter which is assumed driving the motor.

The parameters values of M, T, a and ρ used in the simulation studies are, respectively, 95000, 0.008, 380 and 15. The parameter value of δ shall be fixed to 10^{-8}.

The evolution of $\theta(t)$ with a dynamic design parameter for two scenarios is given in Fig. 4.
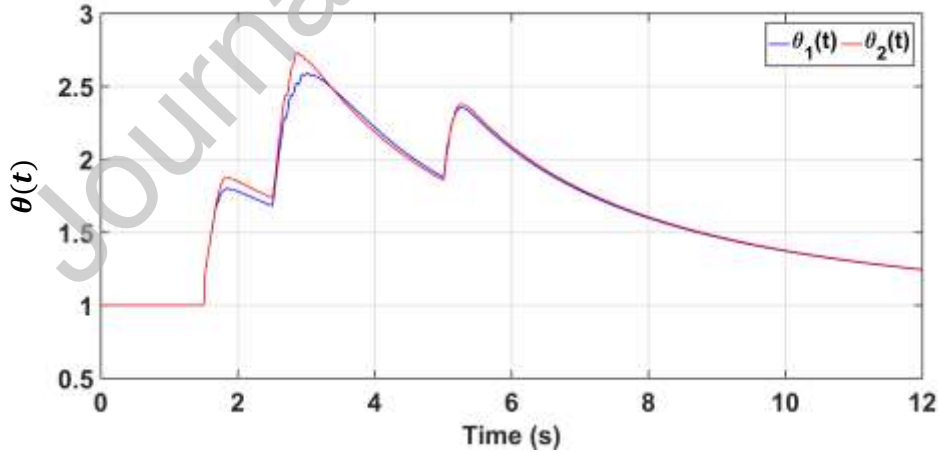
Fig. 4 Evolution of $\theta(t)$ with a dynamic design parameter for two cases

$\theta_1(t)$: without noise, $\theta_2(t)$: with noise

Scenario I: Speed estimation with noise free measurements

As illustrated in Fig. 4, one notices that the value of gain parameter $\boldsymbol{\theta_1(t)}$ increases when the observation errors increase. At these events, decrease of the observation errors induces a decrease of the gain parameter $\boldsymbol{\theta_1(t)}$.

The simulated and estimated rotor shaft speeds are illustrated in Fig. 5. The rotor speed error due to disturbance is very low and rapidly converges to zero after the disturbance induced by the application of load torque as shown in Fig. 6. The estimated torque is shown in Fig. 6.
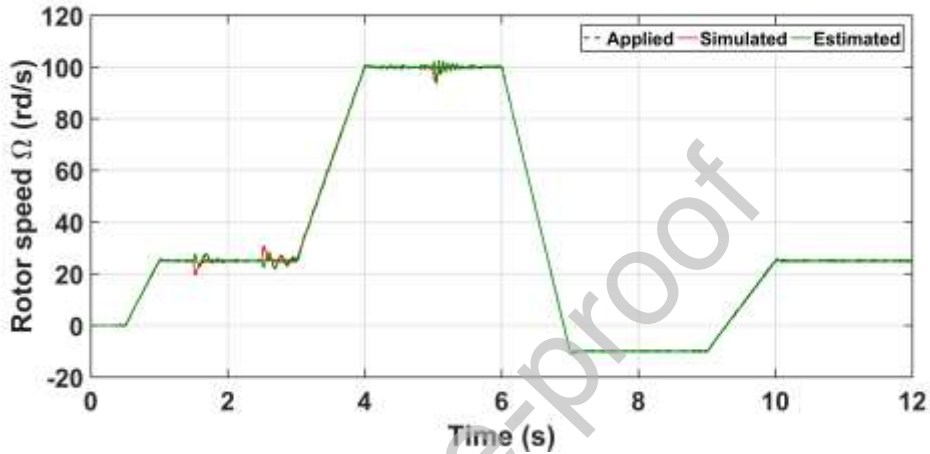
Fig. 5. Simulated and estimated speeds free of noise.
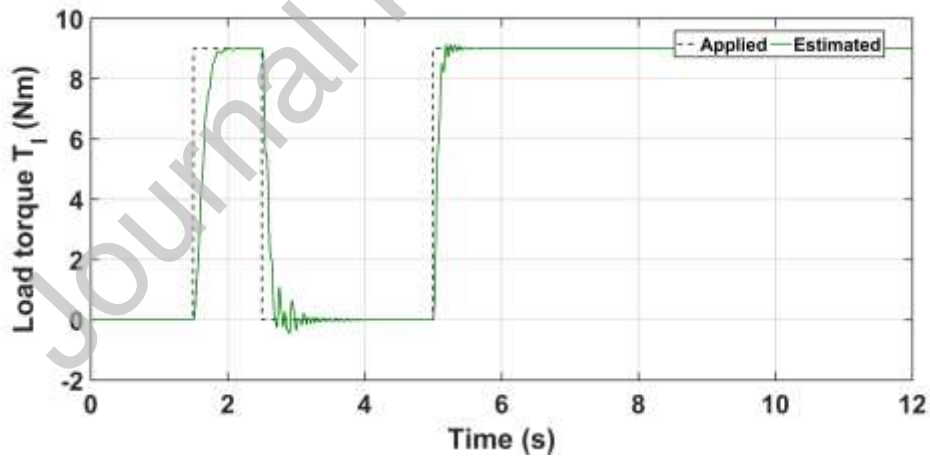
Fig. 6. Estimated total torque free of noise.

Scenario II: Speed estimation in the presence of measurement noise

In this scenario, the results derived from the simulations clearly show that the observer results in a good tradeoff between the sensitivity of measurement noise, and both fast convergence and performance recovery. The time evolution of $\boldsymbol{\theta_2(t)}$ is given in Fig. 4. The graph showing the evolution of the gain

parameter $\boldsymbol{\theta_2(t)}$ has the same shape as the gain parameter $\boldsymbol{\theta_1(t)}$ where the observer works free of noise. However, one notices that the gain parameter $\boldsymbol{\theta_2(t)}$ decreases very quickly, see at time 3 s, compared to the case when the noise is neglected.

The simulated and estimated rotor shaft speeds in the presence of measurement noise are shown in Fig. 7. The rotor speed error due to disturbance is very small and rapidly converges to zero after the load torque variations as shown in Fig. 8. The proposed observer has good performance for the scenario of the presence of measurement noise. As previously mentioned, the proposed observer provides good compromise between the fast convergence of the states, noise rejection and the attenuation of the peaking phenomenon (overshoot problem) as will be seen in the following scenario.
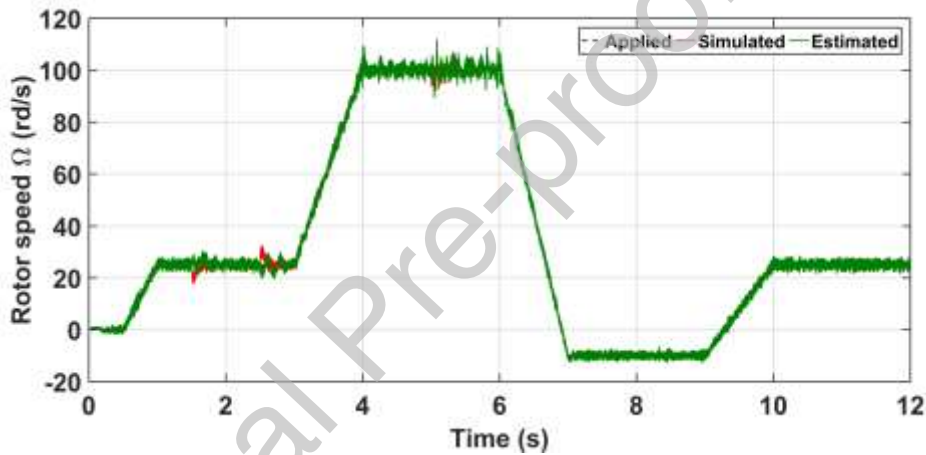
Fig. 7 Simulated and estimated speeds in the presence of the measurement noise.
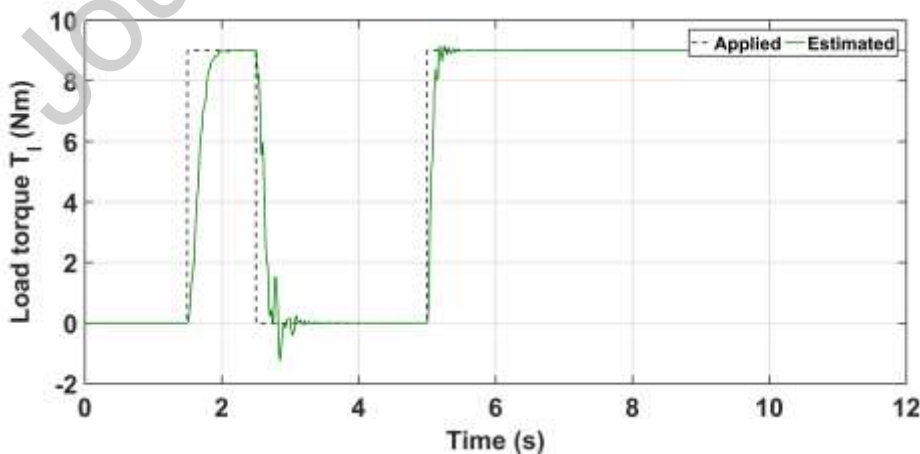
Fig. 8 Estimated total torque in the presence of the measurement noise.

Scenario III Speed estimation considering two constant values for the design parameter $\theta \in \{\theta_{min} = 1,$

$\theta_{max} = 2.73\}$

In this scenario, for comparison the observer is simulated by using tow different values of $\boldsymbol{\theta}$ as follows :

$\boldsymbol{\theta} = \mathbf{1}$ and $\boldsymbol{\theta} = \mathbf{2.73}$. This observer is a standard high gain one [63]. The obtained estimated errors in

the presence of the noisy measurements are shown in Figs. 9 and 10. Note that the value of $\boldsymbol{\theta} = \mathbf{1}$ is too

low to guarantee an accurate estimate, while, $\boldsymbol{\theta} = \mathbf{2.73}$ provides good estimates in cases where no

noise is considered, as shown in Figs. 11 and 12. In the case the output is corrupted by measurement

noise, the obtained estimates are too noisy and peaking phenomenon is exhibited at 8.5 s as shown in

Figs. 9 and 10. This clearly outlines the utility of the dynamic gain observer as shown in Figs. 7 and 8.
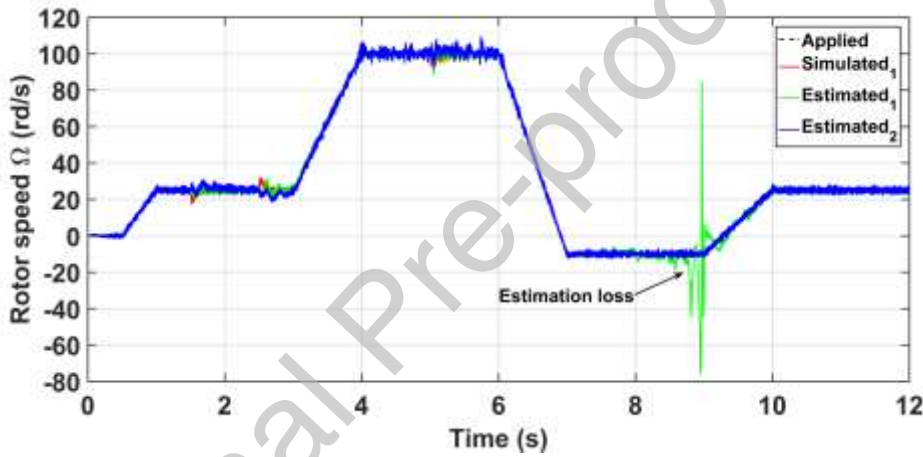
Fig. 9 Simulated and estimated speeds in the presence of the measurement noise. Estimation₁ for

$\boldsymbol{\theta} = \mathbf{2.73}$ and Estimation₂ for $\boldsymbol{\theta} = \mathbf{1}$
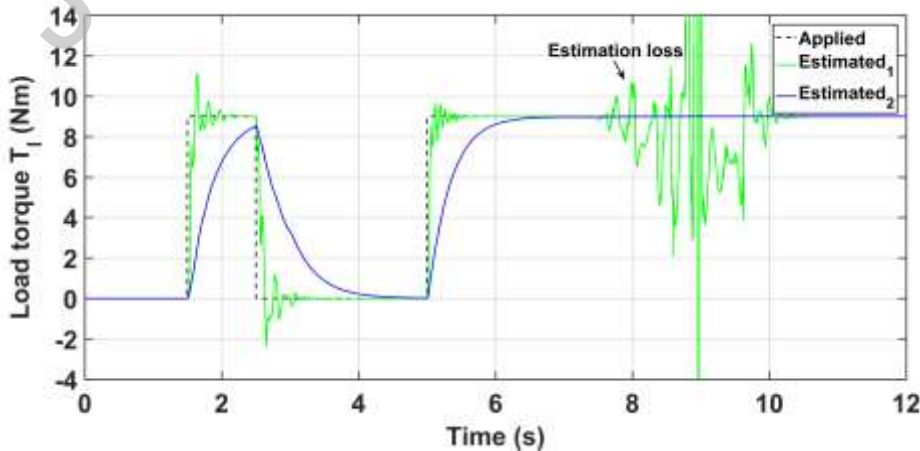
Fig. 10 Estimated total torque in presence of the measurement noise. Estimation$_1$ for $\boldsymbol{\theta} = \mathbf{2.73}$ and
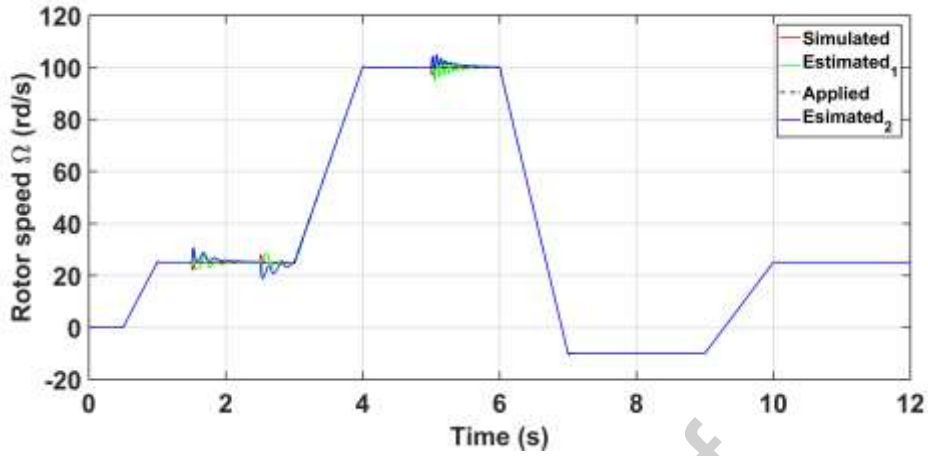
Estimation$_2$ for $\boldsymbol{\theta} = \mathbf{1}$

Fig. 11 Simulated and estimated speeds for noise free. Estimation$_1$ for $\boldsymbol{\theta} = \mathbf{2.73}$ and Estimation$_2$ for

$$\boldsymbol{\theta} = \mathbf{1}$$
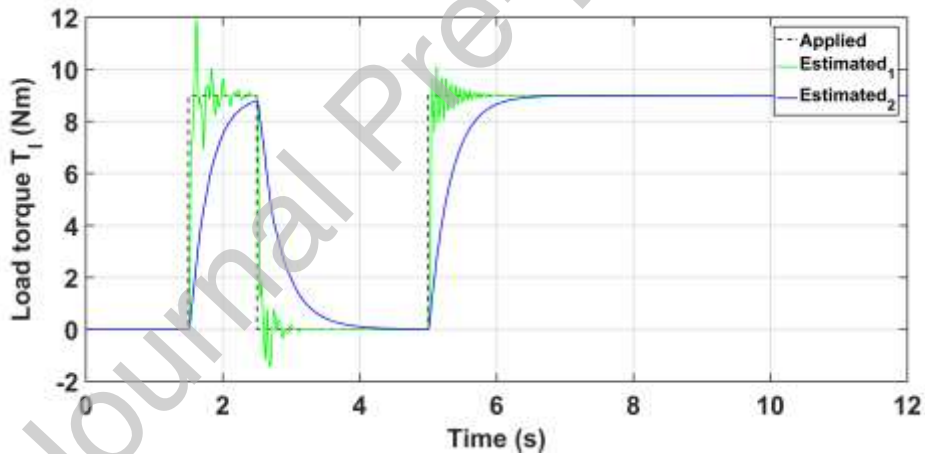
Fig. 12 Estimation error of load torque for noise free. Estimation$_1$ for $\boldsymbol{\theta} = \mathbf{2.73}$ and Estimation$_2$ for

$$\boldsymbol{\theta} = \mathbf{1}$$

conclusions and future work

An efficient nonlinear high gain observer with on-line updating of gain for sensorless speed control of

IMs, using only the measured currents and control voltages in the presence of noise during

measurement, is proposed in this paper. The main idea exploits the proprieties of Riccati differential

equation to find the time-varying parameters that guaranty the best compromise between fast

convergence of the states, noise rejection and attenuation of the peaking phenomenon. Therefore, robustness is also guaranteed under critical working condition, where the standard fixed-gain observer performance deteriorates.

The system mathematical model is presented first and, then, the observability analysis is derived. After that, the design methodology of the proposed observer with updated gain is detailed and its stability verified under large disturbances.

The simulation verification tests are conducted under critical industrial test trajectories and the obtained results demonstrate the effectiveness and robustness of the proposed observer. To further improve the performance and robustness of the proposed observer, future research will involve the generalization of the proposed algorithm to make it suitable to cope with large parameters uncertainties of the induction motors under critical working conditions due to heating, saturation and other physical effects. Moreover, further developments of the proposed algorithm would make it suitable also for applications where an adaptive strategy is needed to overcome system observation uncertainty.

References

[1] J. Holtz, "Sensorless Control of Induction Machines—With or Without Signal Injection?," *IEEE Transactions on Industrial Electronics,* vol. 53, pp. 7-30, 2006.

[2] M. S. Zaky, M. K. Metwaly, H. Z. Azazi, and S. A. Deraz, "A New Adaptive SMO for Speed Estimation of Sensorless Induction Motor Drives at Zero and Very Low Frequencies," *IEEE Transactions on Industrial Electronics,* vol. 65, pp. 6901-6911, 2018.

[3] C. S. Staines, C. Caruana, G. M. Asher, and M. Sumner, "Sensorless control of induction Machines at zero and low frequency using zero sequence currents," *IEEE Transactions on Industrial Electronics,* vol. 53, pp. 195-206, 2006.

[4] G. C. Verghese and S. R. Sanders, "Observers for flux estimation in induction machines," *IEEE Transactions on Industrial Electronics,* vol. 35, pp. 85-94, 1988.

[5] A. Benchaib, A. Rachid, E. Audrezet, and M. Tadjine, "Real-time sliding-mode observer and control of an induction motor," *IEEE Transactions on Industrial Electronics,* vol. 46, pp. 128-138, 1999.

[6] M. Barut, S. Bogosyan, and M. Gokasan, "Switching EKF technique for rotor and stator resistance estimation in speed sensorless control of IMs," *Energy Conversion and Management,* vol. 48, pp. 3120-3134, 2007/12/01/ 2007.

[7] L. Rossignol, M. Farza, M. M'Saad, J. F. Massieu, and R. A. Salas, "OBSERVER DESIGN FOR A CLASS OF NONLINEAR SYSTEMS - APPLICATION TO AN INDUCTION MOTOR," *IFAC Proceedings Volumes,* vol. 35, pp. 339-344, 2002/01/01/ 2002.

[8] A. Maouche, M. M'Saad, B. Bensaker, and M. Farza, "High gain adaptive observer design for sensorless state and parameter estimation of induction motors," *International Journal of Control, Automation and Systems,* vol. 13, pp. 1106-1117, 2015/10/01 2015.

[9] F. Auger, M. Hilairet, J. M. Guerrero, E. Monmasson, T. Orlowska-Kowalska, and S. Katsura, "Industrial Applications of the Kalman Filter: A Review," *IEEE Transactions on Industrial Electronics,* vol. 60, pp. 5458-5471, 2013.

[10] A. Dib, M. Farza, M. M'Saad, P. Dorléans, and J. F. Massieu, "High gain observer for sensorless induction motor," *IFAC Proceedings Volumes,* vol. 44, pp. 674-679, 2011/01/01/ 2011.

[11] M. Ghanes and G. Zheng, "On Sensorless Induction Motor Drives: Sliding-Mode Observer and Output Feedback Controller," *IEEE Transactions on Industrial Electronics,* vol. 56, pp. 3404-3413, 2009.

[12] M. Ghanes, J. D. Leon, and A. Glumineau, "Observability Study and Observer-Based Interconnected Form for Sensorless Induction Motor," in *Proceedings of the 45th IEEE Conference on Decision and Control*, 2006, pp. 1240-1245.

[13] M. Ghanes, J. DeLeon, and A. Glumineau. (2005, Validation of an interconnected high-gain observer for a sensorless induction motor against a low frequency benchmark: application to an experimental setup. *IEE Proceedings - Control Theory and Applications 152(4),* 371-378. Available: https://digital-library.theiet.org/content/journals/10.1049/ip-cta_20045073

[14] W. Sun, X. Liu, J. Gao, Y. Yu, G. Wang, and D. Xu, "Zero Stator Current Frequency Operation of Speed-Sensorless Induction Motor Drives Using Stator Input Voltage Error for Speed Estimation," *IEEE Transactions on Industrial Electronics,* vol. 63, pp. 1490-1498, 2016.

[15] T. Orlowska-Kowalska, M. Korzonek, and G. Tarchala, "Stabilization Methods of Adaptive Full-Order Observer for Sensorless Induction Motor Drive - Comparative Study," *IEEE Transactions on Industrial Informatics,* pp. 1-1, 2019.

[16] S. Suwankawin and S. Sangwongwanich, "Design strategy of an adaptive full-order observer for speed-sensorless induction-motor Drives-tracking performance and stabilization," *IEEE Transactions on Industrial Electronics,* vol. 53, pp. 96-119, 2006.

[17] M. Korzonek, G. Tarchala, and T. Orlowska-Kowalska, "A review on MRAS-type speed estimators for reliable and efficient induction motor drives," *ISA Transactions,* 2019/04/02/ 2019.

[18] W. Sun, Z. Wang, D. Xu, X. Yu, and D. Jiang, "Stable Operation Method for Speed Sensorless Induction Motor Drives at Zero Synchronous Speed With Estimated Speed Error Compensation," *IEEE Transactions on Power Electronics,* vol. 34, pp. 11454-11466, 2019.

[19] M. S. Zaky, H. A. Maksoud, and H. Z. Azazi, "Sensorless induction motor drives using adaptive flux observer at low frequencies," *Engineering, Technology & Applied Science Research,* vol. 8, pp. 2572-2576, 2018.

[20] Y. Wang, L. Zhou, S. A. Bortoff, A. Satake, and S. Furutani, "An approximate high gain observer for speed-sensorless estimation of induction motors," *IEEE/CAA Journal of Automatica Sinica,* vol. 6, pp. 53-63, 2019.

[21] C. Schauder, "Adaptive speed identification for vector control of induction motors without rotational transducers," *IEEE Transactions on Industry Applications,* vol. 28, pp. 1054-1061, 1992.

[22] R. Kumar, S. Das, P. Syam, and A. K. Chattopadhyay, "Review on model reference adaptive system for sensorless vector control of induction motor drives," *IET Electric Power Applications,* vol. 9, pp. 496-511, 2015.

[23] G. Schreier, J. DeLeon, A. Glumineau, and R. Boisliveau. (2001, Cascade nonlinear observers: application to an experimental induction motor benchmark. *IEE Proceedings - Control Theory and Applications 148(6),* 509-515. Available: https://digital-library.theiet.org/content/journals/10.1049/ip-cta_20010641

[24] M. Ghanes, J. D. Leon, and A. Glumineau, "Cascade and high-gain observers comparison for sensorless closed-loop induction motor control," *IET Control Theory & Applications,* vol. 2, pp. 133-150, 2008.

[25] A. Kadrine, Z. Tir, M. A. Hamida, O. P. Malik, A. Houari, and A. E. Aroudi, "High Gain Observer with Updated Gain for Sensorless Induction Motor," in *2018 International Conference on Electrical Sciences and Technologies in Maghreb (CISTEM)*, 2018, pp. 1-6.

[26] Y. Wang, L. Zhou, S. A. Bortoff, A. Satake, and S. Furutani, "High gain observer for speed-sensorless motor drives: Algorithm and experiments," in *2016 IEEE International Conference on Advanced Intelligent Mechatronics (AIM)*, 2016, pp. 1127-1132.

[27] R. E. Kalman and R. S. Bucy, "New Results in Linear Filtering and Prediction Theory," *Journal of Fluids Engineering,* vol. 83, pp. 95-108, 1961.

[28] S. Raghavan and J. K. Hedrick, "Observer design for a class of nonlinear systems," *International Journal of Control,* vol. 59, pp. 515-528, 1994/02/01 1994.

[29] G. Besancon and H. Hammouri, "On Observer Design for Interconnected System," *Journal of Mathematical Systems Estimation and Control,* vol. 8, pp. 1-25, 1998.

[30] A. A. Prasov and H. K. Khalil, "A Nonlinear High-Gain Observer for Systems With Measurement Noise in a Feedback Control Framework," *IEEE Transactions on Automatic Control,* vol. 58, pp. 569-580, 2013.

[31] B. Yi and W. Zhang, "A nonlinear updated gain observer for MIMO systems: Design, analysis and application to marine surface vessels," *ISA Transactions,* vol. 64, pp. 129-140, 2016/09/01/ 2016.

[32] J. P. Gauthier, H. Hammouri, and S. Othman, "A simple observer for nonlinear systems applications to bioreactors," *IEEE Transactions on Automatic Control,* vol. 37, pp. 875-880, 1992.

[33] A. A. Ball and H. K. Khalil, "High-gain observers in the presence of measurement noise: A nonlinear gain approach," in *2008 47th IEEE Conference on Decision and Control*, 2008, pp. 2288-2293.

[34] H. K. Khalil and L. Praly, "High-gain observers in nonlinear feedback control," *International Journal of Robust and Nonlinear Control,* vol. 24, pp. 993-1015, 2014/04/01 2014.

[35] M. Farza, M. Oueder, R. B. Abdennour, and M. M'Saad, "High gain observer with updated gain for a class of MIMO nonlinear systems," *International Journal of Control,* vol. 84, pp. 270-280, 2011/02/01 2011.

[36] H. Hammouri, B. Targui, and F. Armanet, "High gain observer based on a triangular structure," *International Journal of Robust and Nonlinear Control,* vol. 12, pp. 497-518, 2002/05/01 2002.

[37] D. Astolfi, L. Marconi, L. Praly, and A. R. Teel, "Low-power peaking-free high-gain observers," *Automatica,* vol. 98, pp. 169-179, 2018/12/01/ 2018.

[38] V. Andrieu, L. Praly, and A. Astolfi, "High gain observers with updated gain and homogeneous correction terms," *Automatica,* vol. 45, pp. 422-428, 2009/02/01/ 2009.

[39] H. Shim, "A passivity-based nonlinear observer and a semi-global separation principle," Seoul National University, 2000.

[40] F. Esfandiari and H. K. Khalil, "Output feedback stabilization of fully linearizable systems," *International Journal of Control,* vol. 56, pp. 1007-1037, 1992/11/01 1992.

[41] P. V. Kokotovic, "The joy of feedback: nonlinear and adaptive," *IEEE Control Systems Magazine,* vol. 12, pp. 7-17, 1992.

[42] H. K. Khalil, "High-gain observers in nonlinear feedback control," in *2008 International Conference on Control, Automation and Systems*, 2008, pp. xlvii-lvii.

[43]   M. Oueder, M. Farza, R. Ben Abdennour, and M. M'Saad, "A high gain observer with updated gain for a class of MIMO non-triangular systems," *Systems & Control Letters,* vol. 61, pp. 298-308, 2012/02/01/ 2012.

[44]   J. H. Ahrens and H. K. Khalil, "High-gain observers in the presence of measurement noise: A switched-gain approach," *Automatica,* vol. 45, pp. 936-943, 2009/04/01/ 2009.

[45]   M. Montanari, "Discussion on: "Observer Scheme for State and Parameter Estimation in Asynchronous Motors with Application to Speed Control"," *European Journal of Control,* vol. 12, pp. 414-416, 2006/01/01/ 2006.

[46]   S. Hadj Saïd, F. M'Sahli, M. F. Mimouni, and M. Farza, "Adaptive high gain observer based output feedback predictive controller for induction motors," *Computers & Electrical Engineering,* vol. 39, pp. 151-163, 2013/02/01/ 2013.

[47]   S. Hadj Saïd, M. F. Mimouni, F. M'Sahli, and M. Farza, "High gain observer based on-line rotor and stator resistances estimation for IMs," *Simulation Modelling Practice and Theory,* vol. 19, pp. 1518-1529, 2011/08/01/ 2011.

[48]   M. Farza, M. M'Saad, M. Triki, and T. Maatoug, "High gain observer for a class of non-triangular systems," *Systems & Control Letters,* vol. 60, pp. 27-35, 2011/01/01/ 2011.

[49]   A. Neumaier, "Solving Ill-Conditioned and Singular Linear Systems: A Tutorial on Regularization," *SIAM Review,* vol. 40, pp. 636-666, 1998.

[50]   R. Hermann and A. Krener, "Nonlinear controllability and observability," *IEEE Transactions on Automatic Control,* vol. 22, pp. 728-740, 1977.

[51]   H. Nijmeijer and A. Van der Schaft, *Nonlinear dynamical control systems* vol. 175: Springer.

[52]   S. Ibarra-Rojas, J. Moreno, and G. Espinosa-Pérez, "Global observability analysis of sensorless induction motors," *Automatica,* vol. 40, pp. 1079-1085, 2004/06/01/ 2004.

[53]   A. Krener and W. Respondek, "Nonlinear Observers with Linearizable Error Dynamics," *SIAM Journal on Control and Optimization,* vol. 23, pp. 197-216, 1985/03/01 1985.

[54]   J. Rudolph and M. Zeitz, "A block triangular nonlinear observer normal form," *Systems & Control Letters,* vol. 23, pp. 1-8, 1994/07/01/ 1994.

[55]   A. J. Krener and A. Isidori, "Linearization by output injection and nonlinear observers," *Systems & Control Letters,* vol. 3, pp. 47-52, 1983/06/01/ 1983.

[56]   X.-H. Xia and W.-B. Gao, "Nonlinear observer design by observer error linearization," *SIAM J. Control Optim.,* vol. 27, pp. 199-216, 1989.

[57]   J. P. Gauthier and G. Bornard, "Observability for any u(t) of a class of nonlinear systems," in *1980 19th IEEE Conference on Decision and Control including the Symposium on Adaptive Processes*, 1980, pp. 910-915.

[58]   H. Hammouri, "Uniform Observability and Observer Synthesis," in *Nonlinear Observers and Applications*, G. Besançon, Ed., ed Berlin, Heidelberg: Springer Berlin Heidelberg, 2007, pp. 35-70.

[59]   H. Hammouri, F. S. Ahmed, and S. Othman, "Observer design based on immersion technics and canonical form," *Systems & Control Letters,* vol. 114, pp. 19-26, 2018/04/01/ 2018.

[60]   P. Krishnamurthy and F. Khorrami, "Generalized adaptive output-feedback form with unknown parameters multiplying high output relative-degree states," in *Proceedings of the 41st IEEE Conference on Decision and Control, 2002.*, 2002, pp. 1503-1508 vol.2.

[61]   H. Lei and W. Lin, "Universal adaptive control of nonlinear systems with unknown growth rate by output feedback," *Automatica,* vol. 42, pp. 1783-1789, 2006/10/01/ 2006.

[62]   O. Barambones and P. Alkorta, "A robust vector control for induction motor drives with an adaptive sliding-mode control law," *Journal of the Franklin Institute,* vol. 348, pp. 300-314, 2011/03/01/ 2011.

[63]   M. Farza, M. M'Saad, and M. Sekher, "A SET OF OBSERVERS FOR A CLASS OF NONLINEAR SYSTEMS," *IFAC Proceedings Volumes,* vol. 38, pp. 765-770, 2005/01/01/ 2005.